Lund University GEM thesis series nr 24

# Monitoring trends of greenness and LULC (land use/land cover) change in Addis Ababa and its surrounding using MODIS time-series and LANDSAT Data

**Tesfaye Gebeyehu Admasu**

2017
Department of Physical Geography and Ecosystem Science
Lund University
Sölvegatan 12
S-223 62 Lund
Sweden

**To**
**Maedot Tesfaye and Ananeya Tesfaye**

# Monitoring trends of greenness and LULC (land use/land cover) change in Addis Ababa and its surrounding using MODIS time-series and LANDSAT Data

by

Tesfaye Gebeyehu Admasu

---

Thesis submitted to the department of Physical Geography and Ecosystem Science, Lund University, in partial fulfilment of the requirements for the degree of Master of Science in Geo-information Science and Earth Observation for Environmental Modelling and Management

Thesis assessment Board

First Supervisor: Dr. Micael Runnström (Lund University)

Exam committee:
Examiner 1: Professor Lars Eklundh (Lund University)
Examiner 2: Dr. Maj-Lena Linderson (Lund University)

Disclaimer

This document describes work undertaken as part of a program of study at the University of Lund. All views and opinions expressed therein remain the sole responsibility of the author, and do not necessarily represent those of the institute.

Course title: Geo-information Science and Earth Observation for Environmental Modelling and Management (GEM)

Level: Master of Science (MSc)

Course duration: January 20*17* until June 20*17*

Consortium partners:

The GEM master program is a cooperation of departments at 5 different universities:
University of Twente, ITC (The Netherlands)
University of Lund (Sweden)
University of Southampton (UK)
University of Warsaw (Poland)
University of Iceland (Iceland)

## Abstract

NDVI (Normalized Difference Vegetation Index) was introduced in 1974. Despite its limitations, it has been under use for monitoring bio-physical and cultural landscapes from satellite. The present study employed MODIS based NDVI to examine trends of greenness and its link with LULC (land use/land cover) change and rainfall in Addis Ababa and its surrounding (covering 1,217 sq km) over a period of 17 years (2000-2016). Supervised classification of LANDSAT was carried out to identify four thematic classes. Land use land cover change was detected using post classification comparison method. Yearly aggregates of mean, standard deviations (SD), minimum and maximum values of NDVI were generated from MODIS time-series images (n= 387) and spatially mapped. The aggregated yearly NDVI and rainfall values were standardized to z-scores and statistically correlated. The change no-change classes were found to be 427(35%) and 790 (65%) square kilometers respectively. The study revealed an overwhelming increase in built-up area by 183%. Agriculture and vegetation were reduced by 34% and 29% respectively. A general decline in NDVI implying net-loss in greenness was revealed in the study area. Spatio-temporal variation was observed in the onset (start), green up (peak), senescence (decline) and end (dormancy) dates of NDVI. Spatially, three classes of NDVI were identified: low NDVI zone (the center with homogeneous built-up area), medium NDVI zone (the transitional zone with mixed LULC) and high NDVI zone (the periphery with a relatively better vegetation cover). Major land cover change classes were found to be predominantly located in the transitional NDVI zones and slightly in the peripheral zones. NDVI was found to be positively correlated with rainfall data ($R^2$=0.25, Addis Ababa station) and ($R^2$=0.2, Bole station). Nevertheless; the correlation between maximum NDVI and rainfall values has shown a decreasing trend over the years (highly declined after 2010). NDVI decline was found to be earlier (2008/09) in the time-series compared to rainfall (2010/11). The study concludes that decline in NDVI between 2000 and 2016 in the study area is more explained by net-loss in vegetation and agricultural land than decline in rainfall. Ultimately, the study recommends the integration of field based bio-physical and anthropogenic variables with fine spatial resolution remote sensing data for further research.



**Key Words**: Physical Geography and Ecosystem Science, NDVI, Addis Ababa, MODIS, Time-series, Greenness, LULC.

**Acknowledgements**

First, I would like to thank the European Union for providing the Erasmus scholarship to carry out my study in the distinguished European Universities of the GEM consortium: University of Twente (ITC faculty), the Netherlands and Lund University (Department of Physical Geography and Ecosystem Science, Science Faculty), Sweden.

I would like to extend my heartfelt appreciation to my supervisor *Dr.Micael Runnström* for his unreserved and constructive comments throughout the research process.

The board of examiners: *Professor Lars Eklundh* and *Dr.Maj-Lena Linderson* are highly acknowledged for their constructive comments during the evaluation of the thesis.

The instructors involved in delivering courses and administrative secretaries coordinating the GEM program both in ITC and Lund are highly appreciated for their dedication.

Being away from family and kids for the purpose of education is not an easy endeavor. Therefore, I would like to thank my wife *Kiyya* for her motivation, patience, taking care of children and facing all the challenges during my absence. *Kiyye, Filoo, Babiye,* I love you!!!

I would like to thank members of my family, *especially my mother Bekelech Mekonnen and my sister Firehiywot Mekonnen*; who have made their contribution for caring my wife and kids in all the challenges they faced during my absence.

The relentless help from my close friend *Ashenafi Tilahun* during field work is highly valued.

Ato *Samuel Tilahun* and my uncle *Yitna* are highly acknowledged for facilitating access to climatic data during field work.

The workers of Gulele Botanical Garden in Addis Ababa, *especially Wondiye Kebede*; are acknowledged for their cooperation.

Friends and classmates of the 2015-2017 cohort: MSc students of Natural Resources Management (ITC) and MSc students of Geo-Information Science and Earth Observation (GEM) are remembered for facing the academic challenge and sharing the fun part of it together.

Above all, I would like to say thanks to GOD who has been with me and helpful throughout all my journey in this world!!!

## Table of Contents

**List of Tables**



**List of Figures**

## List of Abbreviations

a.m.s.l: Above Mean Sea Level

AACA: Addis Ababa City Administration

AACAILIC: Addis Ababa City Administration Integrated Land Information Center

AOI: Area of Interest

AVHRR: Advanced Very High Resolution Radiometer

DN: Digital Numbers (pixel values)

ETM: Enhanced Thematic Mapper

EVI: Enhanced Vegetation Index

GBG: Gulele Botanical Garden

GIS: Geographic Information Science

IHDP: Integrated Housing Development Program

LULC: Land Use Land Cover

mm: Millimeters

MODIS: Moderate Resolution Imaging Spectroradiometer

MVC: Maximum Value Composite

n.d.: No Date

NASA: National Aeronautics and Space Administration

NDVI: Normalized Difference Vegetation Index

NIR: Near Infrared Region in Electromagnetic spectrum

NMA: National Meteorological Agency

OLI: Operational Land Manager

RED: Red Region in Electromagnetic Spectrum

RS: Remote Sensing

SD: Standard Deviations

sq km: Square Kilometers

TM: Thematic Mapper

UN: United Nations

USGS: United States Geological Survey

VI: Vegetation Indices

# Chapter One: Introduction

## 1.1. Background

In today's world, more people live in urban areas than the rural counterpart. The total population living in urban areas has increased dramatically from 30% in 1950 to 50% in 2007 and 54% in 2014. By 2050, 66% of the world's population is projected to be urban (UN 2014). Developing countries in Africa and Asia are fast urbanizing even though they started the process of urbanization lately (Daniels 2004; UN 2016; UN 2014).

Ethiopia's urban population has grown from 1.6 million (7.5 % of the total population) in 1967 to 4.3 million (11.4% of the total population) in 1984, 7.8 million (14.6% of the total population) in 1994 and then to 16% in 2007 (Gebeyehu 2015). These figures clearly show that the country is least urbanized compared to other regions of the world. Nevertheless; the country has witnessed a relatively rapid urbanization with an annual growth rate of 3.49 %, particularly; after the 1990s (UN-Habitat 2011).

Addis Ababa, the capital city of Ethiopia, was founded in 1886 by Menelik II. Since then, it has been serving as the socio-economic and political hub of the country. Three main factors helped the city to stay as the capital city of Ethiopia: the introduction of eucalyptus (a tree that grows very fast and provides a lot of wood for energy and cooking), the proclamation for legalizing private ownership of urban land in 1907 and the completion, mainly by the French, of the Addis Ababa-Djibouti railway in 1917 (Tolon 2008).

Addis Ababa was emerged as a defense headquarter but without any formal city planning. A number of master plans were made to modernize it. However, most of the plans were not fully implemented as anticipated. Negligible implementation of the master plans was not without consequence. It has greatly contributed to the multi-faceted challenges that are now prevalent in the city (Elias 2008; Yirgalem 2009). The city occupies the central part of Ethiopia and its population is disproportionately large compared to the rest of urban centers in the country. In 2011, for example; its population was 3.4 million which was ten times larger than the second biggest urban center called Dire Dawa (UN-Habitat, 2011). The population is projected to grow by 3.8% per year. This growth is set to continue in the coming 15 years and the total population of the city is projected to be 4.7 million by 2030 (AACA 2009).

Mal-functioning master plans coupled with rapid population growth introduces a multi-faceted challenges to the city of Addis Ababa and its surroundings. One of these challenges are regulated and/or spontaneous land use/land cover changes (LULC) which actually happen at the expense of environmental assets, namely; vegetation within the city and/or in its surrounding. Besides, urban areas exhibit environmental impacts that extend beyond city boundaries: urban heat island effects, impervious surfaces that alter sensible and latent heat fluxes, conversion and fragmentation of natural ecosystems, loss of agricultural land, contamination of air, soil and water, increased water use and runoff, and reduced biodiversity (Schneider et al. 2010; UN 2016).

Developing accurate, consistent and timely data on trends in urbanization and city growth are pivotal for assessing current and future needs with respect to urban growth and the associated impacts and thereby to promote sustainable urban and rural development (UN 2014; Gebeyehu 2015). In this regard, the use of remote sensing (RS) data for monitoring the urban and rural setting is pivotal, because; it provides timely and first hand information which would help the proper management of the physical and cultural landscapes.

This thesis, is therefore; aimed at identifying the trends of greenness and LULC change in the light of rapid urbanization using MODIS time-series and LANDSAT data.

## 1.2. The Research Problem

The study of vegetation phenology at global or regional levels is pivotal because it is a sensitive indicator of climate changes and it regulates carbon, energy and water fluxes between the land and atmosphere (Adole, Dash, & Atkinson, 2016;  Xuanlong et al. 2012; Zhang et al. 2003). Phenological properties, such as the timing and rate of green-up, amplitude and duration of the vegetation growth, and timing and rate of vegetation senescence have become emerging indicators of global environmental changes (Suepa et al. 2016).

The use of satellite observations has been to either to track trends in the greenness of vegetation through time, primarily as an indicator of ecosystem response to changes in climate or to understand the effect of human activity on landscapes. Particularly in urban environments, human actions can lead to either increases or decreases in vegetation greenness. For example, conversion of agricultural land or forests to developed land usually results in a decrease in vegetation greenness. Conversely, planting of vegetation in urban environments is a common element of urban planning and can lead to increases in greenness (Zhu et al. 2015).

Changes in vegetation occur in either of the three ways: a seasonal or cyclic change which is induced by climate such as annual temperature and rainfall, impacting plant phenology; a gradual change over time such as change in land management or land degradation; and an abrupt shift at a specific point in time which may be caused by disturbances such as a sudden change in land use policies, deforestation, floods, droughts, and fire (Teferi, Uhlenbrook, & Bewket, 2015). Similarly, Tadesse et al. (2014) and Yengoh et al. (2015) have noted that caution has to be made while analyzing RS data, because; anomaly are either caused by environmental stress (flooding, fire, pest infestation and hail damage) or anthropogenic causes (land conversions).

Fetene & Worku (2013) have analyzed LULC and functional forest zones in the upper catchment of Addis Ababa using multi-temporal TM/ETM$^+$ (1986, 2000 and 2011) and revealed poor species diversity due to anthropogenic impacts and monoculture plantation strategies. Besides, their study has shown density variation between species and poor regeneration potential. This study is limited in scope, because; it has analyzed LULC within the protected area to the North of Addis Ababa. Feyisa et al. (2016) has dealt with urbanization-induced LULC, surface thermal intensity and its relationship with biophysical composition using TM and ETM$^+$. This study revealed surface heat intensity contrast that outskirts are cooler than urban centers by 3.7°C between 1985 and 2010.

Remote sensing based studies conducted on Addis Ababa were either too specific or vary in scope (limited use of time-series data; over emphasize on LULC and so on).

The link between urbanization induced LULC with trends of greenness using remotely sensed data has not been studied adequately in the context of Addis Ababa.

Therefore, the aim of this study is to identify trends of greenness and LULC change using MODIS time-series, LANDSAT 7 $ETM^+$ and LANDSAT 8 (OLI). The study also tries to establish link between NDVI and rainfall data.

### 1.2.1. Specific Objectives of the Study

- To identify trends of greenness and its spatio-temporal variation in Addis Ababa and its surrounding between 2000 and 2016.
- To detect LULC change classes and describe their connection with trends of NDVI over a period of 17 years in the study area.
- To establish link between trends of rainfall and MODIS based NDVI in the study area.

### 1.2.2. Research Questions

- What does the trends of greenness and its spatio-temporal variation look like in Addis Ababa and its surrounding between 2000 and 2016?
- What are the major LULC change classes in the study area and how are they related to NDVI trends over a period of 17 years in the study area?
- Does field based rainfall and satellite based NDVI correlate?

## 1.3. Scope of the Study

This study is delimited to Addis Ababa and its surrounding, Ethiopia. It mainly focuses on monitoring trends of greenness and LULC using MODIS time-series, LANDSAT 7 $ETM^+$ and LANDSAT 8 (OLI) over a period of 17 years.

## 1.4. Limitations of the Study

Land cover classification using bi-temporal remote sensing images is the most common method for monitoring of LULC change over the surface of the earth. Nevertheless; bi-temporal images used for detecting changes greatly depend on the research objectives and the nature of changes (gradual or abrupt) in the physical and/or anthropogenic environment. Remote sensing images with 5 to 10 years interval are usually considered for detecting LULC changes over time. This study, however; employed two images (2000 and 2017) with an approximately 17 years time interval. Thus; using multi-temporal images with 5 to 10 years interval would yield a better classification information. Besides, higher spatial resolution images might help to enhance the accuracy of the classification.

The present study tries to examine trends of greenness in Addis Ababa and its surrounding using MODIS time-series data. Trends of greenness was analyzed based on mean, maximum, standard deviations (SD) and minimum values of NDVI derived from MODIS averaging the whole study area. Therefore; considering a homogenously vegetated and/or agricultural area separated from a highly mixed urban area would help to capture trends of NDVI for each land cover classes. These issues need to be considered for further research.

# Chapter Two: Literature Review

## 2.1.Vegetation Indices and Phenology: An Overview

Vegetation indices (VI) are dimensionless measures derived from radiometric data that are primarily used to indicate the amount of green vegetation present in the view (Jones and Vaughan, 2010). They are optical measures of vegetation "greenness" and quantifies vegetation amount and health through the combined measurements of the chlorophyll absorbing RED spectral region (0.6–0.7 μm) with the non-absorbing, leaf reflectance signal in the near-infrared (NIR) (0.7–1.3 μm) to provide a consistent and vigorous measure of area averaged canopy photosynthetic capacity (Huete 2014). Though most VIs use NIR and RED bands for explaining vegetation phenology, there are possibilities of using the other bands too (Jones and Vaughan, 2010).

Using VIs is an efficient, seamless and robust approach for monitoring plant phenology from remotely sensed data (Jin & Eklundh 2014; Huete et al. 2014). They are among the most widely used satellite products, providing key measurements in productivity, phenology, climate, hydrology, biogeochemical and biodiversity studies (Huete et al. 2014).

Scientists have extracted and modeled a variety of biophysical variables and algorithms for studying vegetation since the 1960s. In today's world, it is believed that there are many more remote sensing based indices for studying vegetation (Jensen 2000).

Vegetation Phenology inferred from remote sensing is characterized by four key transition dates, which define the key phenological phases of vegetation dynamics at annual time scales. These transition dates are: (1) green-up, the date of onset of photosynthetic activity; (2) maturity, the date at which plant green leaf area is maximum; (3) senescence, the date at which photosynthetic activity and green leaf area begin to rapidly decrease; (4) dormancy, the date at which physiological activity becomes near zero (Zhang et al. 2003). Vegetation phenology can be characterized through the study of rate of increase or decrease of NDVI, dates of the beginning or end of the growing season, length of the "green" season, and timing of the annual maximum NDVI (Pettorelli et al. 2005).

Vegetation phenology can be studied using field based in-situ measurements, remote sensing based methods or a combination of both. A general concern for all ground-based measurements globally, is the evident lack of a standard approach to measuring vegetation phenological stages. Using in-situ field techniques, ground-based measurements can provide detailed and fine temporal resolution data on plant phenology, although these data may suffer from very limited spatial coverage (Adole et al. 2016).

The variables which could be derived from time-series RS data can be categorized in to five major classes, namely; geophysical variables, index variables, thematic variables, topographic variables and texture variables as shown in Table 2.1. The analysis of time series remote sensing data basically depends on raw digital numbers (DN) reflectance values (in%) (Claudia, Stefan and Wolfgang 2015). In this research, nevertheless; emphasis was made on the index variables, namely NDVI.

*Table 2.1. Measurable variables of time-series remote sensing data*

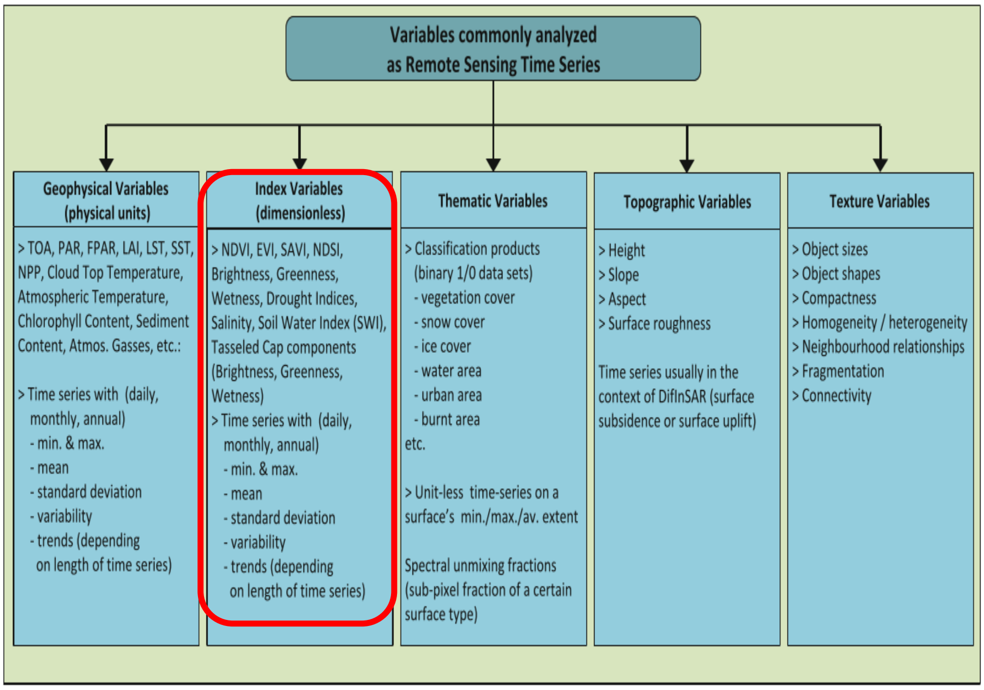


*Source: (Claudia, Stefan and Wolfgang 2015).*

## 2.2.Vegetation Indices

### 2.2.1. NDVI (Normalized Difference Vegetation Index)

NDVI is the calculated based on spectral responses of vegetation (reflectance) in the NIR (near infrared) and RED bands. It is a normalized transform of the NIR and RED reflectance ratio (Huete et al. 2002; Yengoh et al. 2015). The NDVI algorithm takes an advantage of the fact that green vegetation reflects less visible light and more NIR, while sparse or less green vegetation reflects a greater portion of the visible and less near-IR (Yengoh et al. 2015).

NDVI is expressed as a function of reflectance and calculated using the algorithm in equation 1 (Rouse et al. 1974):

$$NDVI = \frac{\rho NIR - \rho red}{\rho NIR + \rho red} \qquad \text{Eq. 1}$$

The range of values obtained from the algorithm is between −1 and +1. Only positive values correspond to vegetated zones. The higher the index value the greater the chlorophyll content or greenness of the target and vice versa. NDVI has been successful for monitoring inter-annual vegetation growth and their phenological changes. The ratioing of NIR and RED bands also reduces multiplicative noise (illumination differences, cloud shadows, atmospheric attenuation, and certain topographic variations) which is apparent in multi-band and multi-date images. However, NDVI is highly sensitive to differences in canopy background and asymptotic (saturated) signals over high biomass conditions (Jensen 2000; Huete et al.

2002). Regardless of its limitations, the NDVI algorithm has continued to be used for monitoring of natural and anthropogenic landscapes using various sensors like LANDSAT, AVHRR, MODIS and so on. In the mean time, a number of new indices have been derived based on NDVI to increase the interpretability of satellite images.

### 2.2.2. EVI (Enhanced Vegetation Index)

EVI was developed to offset the limitations related to NDVI: to be more sensitive to changes in areas having high biomass; reduce the influence of atmospheric conditions on vegetation index values, and correct for canopy background signals (Huete et al. 2002; Jensen 2000).

The algorithm takes the form

$$EVI = G \frac{\rho NIR - \rho red}{\rho NIR + C_1 \times \rho red - C_2 \times \rho blue + L} \qquad \text{Eq. 2}$$

Where; $\rho$ is atmospherically corrected or partially atmosphere corrected (Rayleigh and ozone absorption) surface reflectance, $L$ is the canopy background adjustment that addresses nonlinear, differential NIR and red radiant transfer through a canopy, and *C1*, *C2* are the coefficients of the aerosol resistance term, which uses the blue band to correct for aerosol influences in the red band. The coefficients adopted in the EVI algorithm are, $L$=1, $C_1$ =6, $C_2$ =7.5, and $G$=2.5.

Therefore, the EVI algorithm greatly helps to make a clear distinction between the 'green signals' from 'mixed signals' and allows for meaningful spatio-temporal comparison of vegetation activity compared to NDVI.

## 2.3. Land Use Land Cover (LULC)

The concepts of land use and land cover are overlapping. According to Lillesand, Kiefer & Chipman (2015), even if the two terms are used interchangeably they refer to fundamentally different concepts. For example; satellites capture a snapshot of the Earth at a certain point in time which can be expressed as land cover: cornfields, lakes, trees, concrete, and so on. The same land cover will have a land use category from economic function point of view. Similarly, Westinga (2004) has pointed out that remotely sensed data from aerial photographs or satellite images are influenced by the land cover and used to map land cover. This is also helpful to mapping land use since the type and state of the cover found often reflect the land use. In this study, therefore; the two terms will be used interchangeably emphasizing on the concept of land cover in mind.

## 2.4. LULC Classification and Change Detection

LULC change in urban area is a complex process (De Paul, 2007; Sivakumar, 2014). These changes result from natural and/or anthropogenic causes (Yuan et al. 2005). Therefore, accurate detection of changes is pivotal to understand the interplay between natural and human-related phenomena and helps to ensure better use of resources (Lu et al. 2009; Yuan et al. 2005).

Urban monitoring involves: land use change detection and; land use impact analysis. Detecting LULC change deals with identifying the type, proportion/size, and location of changes. land use impact analysis exhibits evaluating the effects of such changes on environment (De Paul, 2007).

Land cover classification using bi-temporal remote sensing images is the most widely used approach for monitoring of changes over the surface of the earth. The basic image classification techniques are: supervised classification, unsupervised classification, and object based classification (Jones & Vaughan, 2010). In this study, however; supervised classification will be used. Visual image interpretation will be employed as a supplement the classification process.

Supervised image classification involves identifying sample pixels with similar spectral properties over the image and training the computer/software to do the rest of the classification based on the sampled pixels over the entire image (Lillesand, Kiefer & Chipman 2015).

For detecting changes in LULC based on LANDSAT data, post classification comparison technique will be employed in this study. Post classification comparison is a method of classifying bi-temporal images into thematic maps separately and then comparing of the classified images pixel by pixel. The accuracy of the resultant maps highly depends of the quality of the classified images in each date. This method is advantageous in that it reduces the impacts of atmospheric, sensor and environmental differences between bi-temporal images and provides a complete matrix of change information (Lu et al. 2009).

### 2.6. Validation of the Classified Image

The accuracy of a supervised classification highly depends on how training samples are well distributed for each classes, the spectral homogeneity of training samples and the positional accuracy of the training samples over the image (Jones & Vaughan 2010; Lillesand, Kiefer & Chipman 2015). Similarly, the following factors should be considered for properly reporting the accuracy of a classified image: ground-truth data, classification scheme, sampling scheme, spatial autocorrelation, and sample size and sample unit (Lu et al. 2009). It was suggested that at least 50 samples of each land cover categories to be included in the error matrix (Lillesand, Kiefer & Chipman 2015).

Image classification is not complete until the accuracy of the land cover classes is assessed using what is called error matrix. Error matrix/confusion matrix compares the relationship between known reference data (ground truth) and the corresponding result from an automated classification process (Lillesand, Kiefer & Chipman 2015). An error matrix helps to validate the accuracy of the classified image and is usually expressed as percentage. An error matrix is interpreted using overall accuracy, user's accuracy, producers accuracy and sometimes kappa statistics. Kappa statistics is the measure of the difference between the actual agreement between reference data and an automated classifier and the chance agreement between the reference data and a random classifier (Lillesand, Kiefer & Chipman 2015).

# Chapter Three: Research Methodology

## 3.1. The Research Setting: Location, Climate and Population

Addis Ababa occupies the central part of Ethiopia and has been serving as the socio-economic and political capital of the country since its establishment in 1886. It is located between 8°45′00″ to 9°05′00″ N and 38°35′00″ to 38°55′00″E (Figure 3.1). Its altitude ranges from 2100 meter at Akaki (South) to 3000 meter at *Entoto* (North) (Fetene & Worku 2013). The average altitude of the city is 2380 meters (a.m.s.l) (Feyisa et al. 2016). The city receives its maximum rainfall in the months of *June, July August* and *September*, the main rainy season, in most parts of the country (Figure 3.2) (NMA n.d.). Maximum monthly temperature is recorded in *March, April* and *May* (Figure 3.3). The mean annual temperature ranges from 16°C to 18°C (appendix 8). Addis Ababa receives an average rainfall of 1255 mm per year (Feyisa et al. 2014). The study area covers 1,217 sq km.

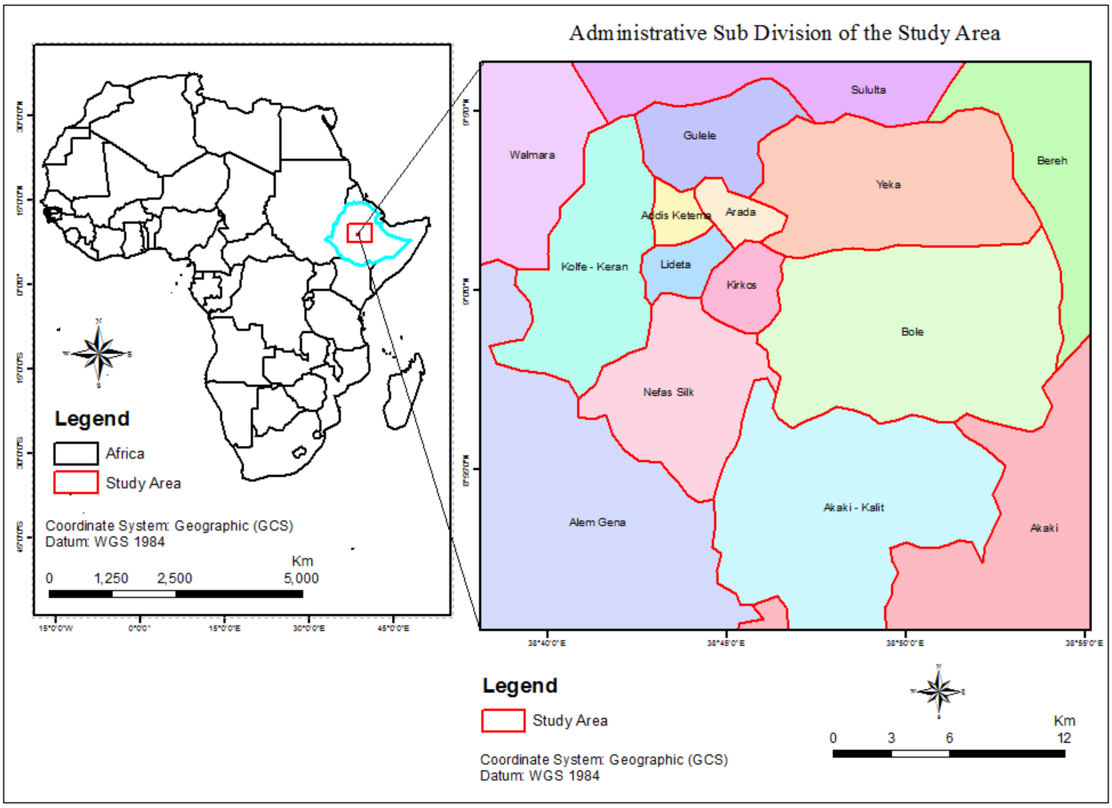

*Figure 3.1 Location of Addis Ababa and its surrounding*

The population of Addis Ababa has grown from 1.4 million in 1984 to 2.1 million in 1994 and then to 2.7 million in 2007 (AACA 2009). This growth is mainly caused by rural-urban migration. The migrant population in the three consecutive census years were 52%, 47% and 48% respectively (Wubneh 2013). In response to decentralization policy adopted by the national government, the percentage of urban population in Addis Ababa has declined from 40% in the 1980s to 25-30% today (Wubneh 2013; Yusuf, Tefera & Zerihun 2009). Nevertheless; the population of the city has been increasing in quantitatively (Figure 3.4). As described in the background part, the rate of urbanization in Addis Ababa is one of the fastest in sub-Saharan Africa with an annual growth rate of 3.8%. Compared to other urban centers in Ethiopia, Addis Ababa continued to be a disproportionately primate city. There is an evidence that the second largest city in the country (Dire Dawa) is 12 times less than Addis Ababa (Wubneh 2013).

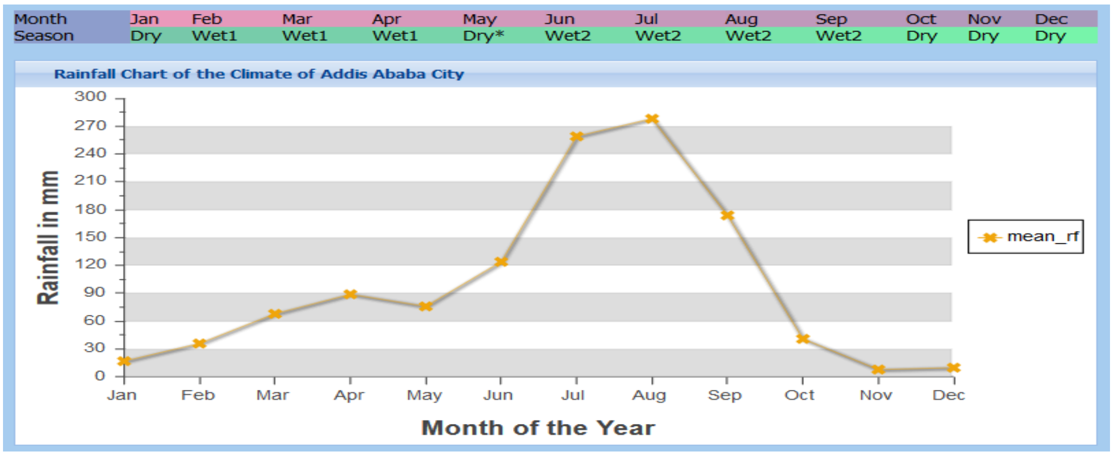


*Figure 3.2. Monthly average rainfall in Addis Ababa (Source: NMA)*

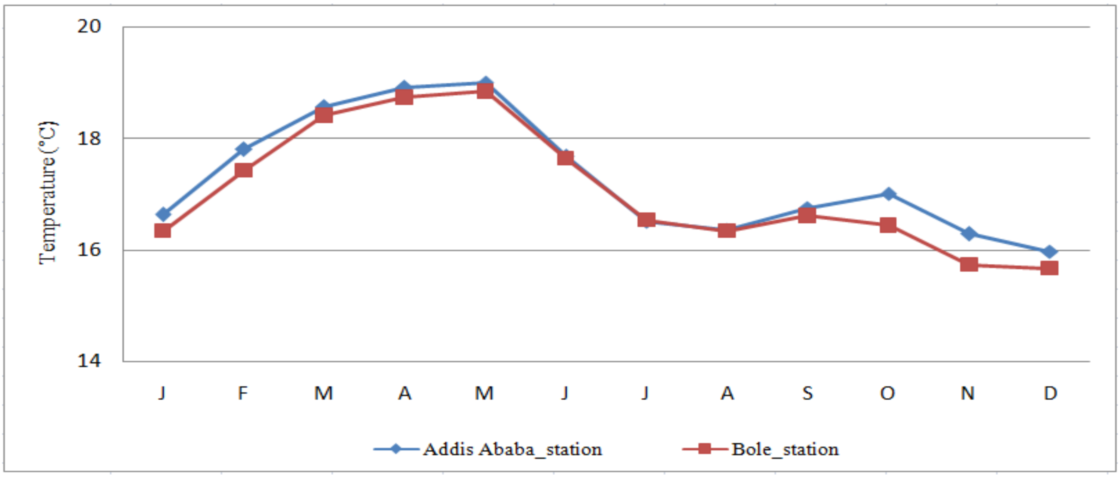


*Figure 3.3. Monthly mean temperature (°C) in Addis Ababa (2000-2015)*

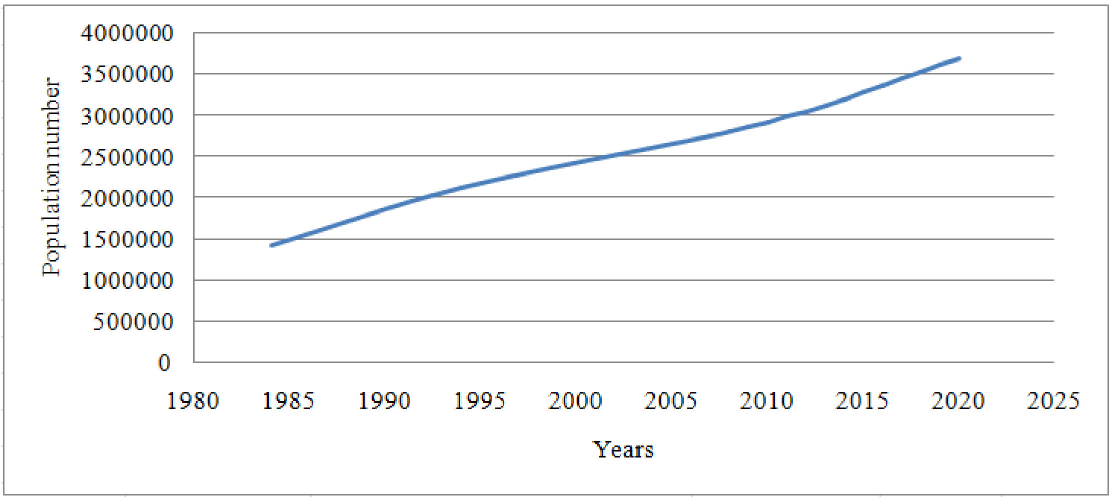


*Figure 3.4. Trends of population growth in Addis Ababa (1984-2020)*

### 3.2. Data Sources and Processing

### 3.2.1. LANDSAT Data and Processing

For detecting LULC, this study employed remote sensing products of LANDSAT 7 $ETM^+$ and LANDSAT 8 (OLI). First, cloud free and atmospherically corrected bi-temporal images (December 05, 2000 and March 15, 2017) with *path 168* and *row 054* were downloaded from the USGS website. The two dates were selected to minimize the impact of clouds during interpretation. Besides, these images help to get a clear picture of LULC in Addis Ababa and its surrounding and reduces confusion during image classification. Since agricultural crops have the same spectral reflectance characteristics like vegetation, it might be confusing if summer season images were used. The images were visually interpreted and pre-processed and made ready for classification and analysis. Four thematic LULC classes (built-up, vegetation, agriculture, and water) were generated for the years 2000 and 2017 using supervised image classification.

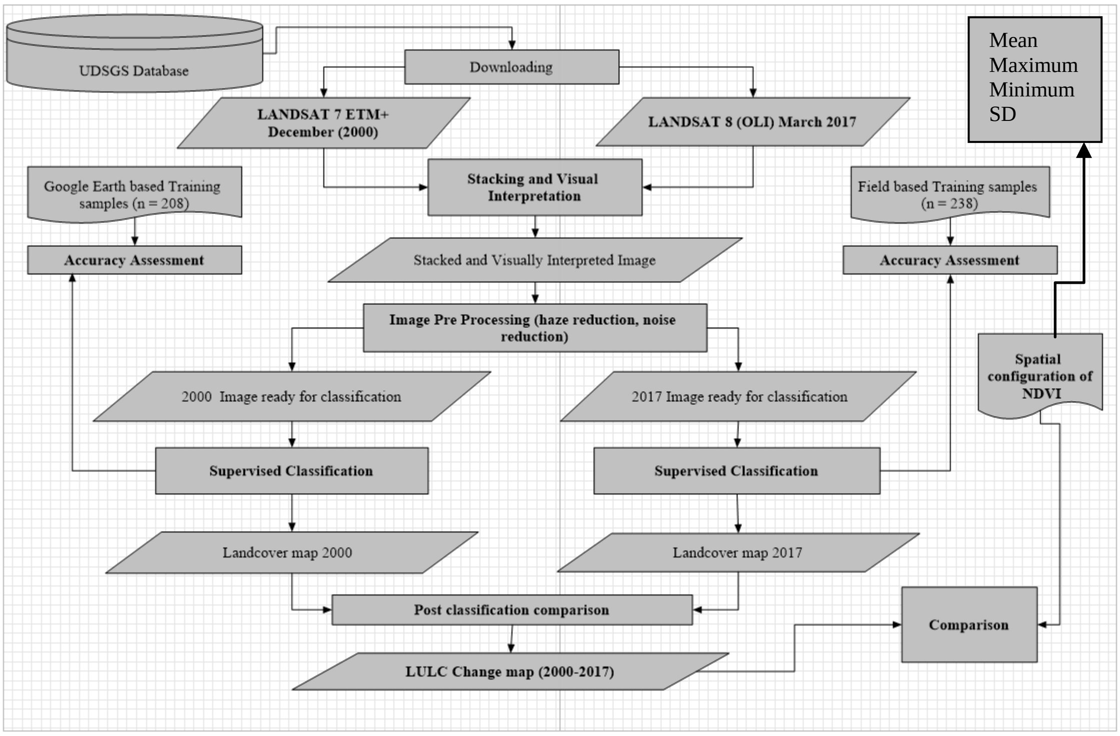


*Figure 3.5. Procedures for processing LANDSAT data*

Accuracy of the classification were checked using 238 sample validation points (Appendix 2 and Appendix 10) which were collected using GPS from the field (March 25-30) for the year 2017. Validation points were collected using stratified random sampling techniques. This sampling technique is selected, because; it considers each land cover class as a stratum from which sample validation points are generated (Lillesand, Kiefer & Chipman 2015).

In order to check the accuracy of thematic LULC classification for the year 2000, there was lack of historical images or topographic maps covering the geographical extent of the current study. Therefore, 208 random sample points (Appendix 1 and Appendix 9) were generated from LANDSAT 7 $ETM^+$ guided by the Google Earth's imagery archive of the same year. Confusion matrix was used to interpret whether the pixels are correctly classified or not. The level of classification accuracy were discussed using *overall accuracy, user's accuracy, producer's accuracy and kappa statistics*. Finally, LULC change was detected using post classification comparison method and Change map was produced. The procedures for pre-processing and processing of LANDSAT images is presented in Figure 3.5.

### 3.2.2. MODIS Data and Processing

MODIS data is used to identify yearly NDVI profile and trends of greenness in the study area over the time series years (2000-2016). MODIS (Moderate Resolution Imaging Spectroradiometer) is an instrument on aboard of the Terra (EOS AM) and Aqua (EOS PM) satellites. Terra MODIS and Aqua MODIS together are able to view the entire earth's surface every 1–2 days (Xie et al. 2008). MODIS product with vegetation indices is available with 36 bands three spatial resolutions, namely; 250m, 500m, and 1 km. MODIS VIs are produced in tile units (10°*10° lat/long) that are approximately 1200-by-1200 km (4800 rows and 4800 columns), and mapped in the Sinusoidal (SIN) grid projection. The radiometric and geometric properties of MODIS onboard NASA's Terra spacecraft is characterized by improved atmospheric correction and cloud screening as provided by MODIS (Zhang et al. 2003).

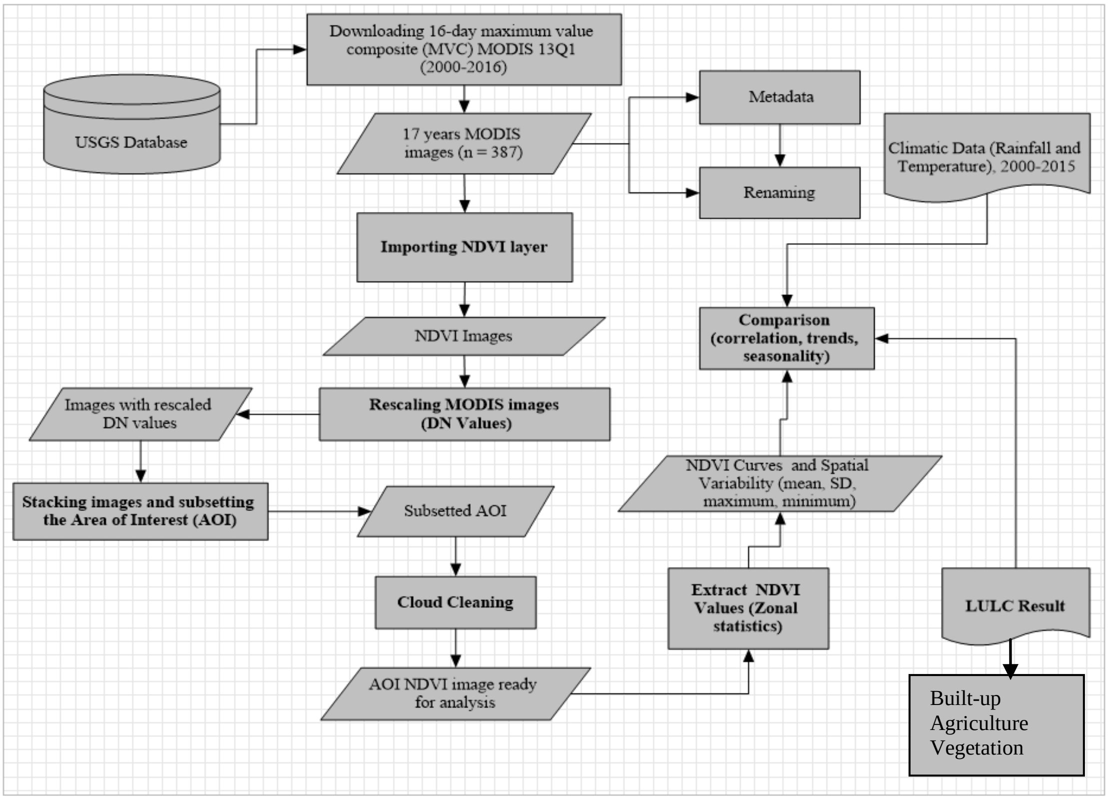


*Figure 3.6. Procedures for processing MODIS data*

For the purpose of this study, MODIS13Q1 MVC (Grid SIN V005; h21v08) images with 16-day repeat cycle and 250 meter spatial resolution were used. Accordingly, 17 years data with 250 meter resolution [from 2000 to 2016] were downloaded (23 images per year and a total of 387 HDF images covering tile unit h21v08) from USGS website: https://lpdaac.usgs.gov. All the 387 layers of MODIS were used as an input for analysis to examine the full trends in greenness and its spatio-temporal variability in the time-series years under consideration. Pixels covering the study area (201 rows and 91 columns) were used the purpose of this research . NDVI was used as an index to monitor trends of greenness in the study area.

Preprocessing of time-series imagery is important when the remotely sensed area covers many images, because; it is important to make these images compatible spatially and spectrally (Xie et al. 2008). Besides, preprocessing helps to reduce noise and increases the accuracy of image interpretation. Cognizant of this, the downloaded images were pre-processed (noise reduction; radiometric correction, geometric correction; enhancement and etc) using the methodological procedures indicated in Figure 3.6 and using the relevant software tools [Erdas Imagine 2016; Envi (IDL) with its extensions; Arc GIS 10.3; R-Studio; Microsoft Excel, Total Commander and so on].

Then, trends of greenness was analyzed for Addis Ababa and its surrounding using annual NDVI time series data from MODIS. Statistical values of NDVI (mean, minimum, maximum, and standard deviation) were extracted and analyzed. In the mean time, NDVI and rainfall based spatio-temporal variability and seasonal trends were compared using Z-score values. Statistical values of NDVI over the study area was generated using zonal statistics algorithm. Zonal statistics is one of the spatial analysis tool and helps to summarize values of a raster within the area of interest (Dell 2009).

Furthermore, the results obtained from MODIS were correlated with climatic data, mainly of rainfall. Ultimately, the overall result of the study was discussed and validated with the results of other similar studies. Eventually, conclusions and future research directions were drawn from the overall analysis.

#### 3.2.2.1. Decomposition and Smoothing of MODIS Time-Series

Satellite image time-series data contains the seasonal, trend and the random/noise component. The seasonal and trend components are principal elements of time-series analysis (Kong et.al. 2015). Therefore; decomposition procedures in time-series are very helpful to separate the trend and seasonal factors from random noise in the time-series. In this paper, additive decomposition method was used assuming constant seasonal change over time in the study area (appendix 3). Additive decomposition presupposes that time-series data is the sum of the seasonal, trend and random components (Prema & Rao, 2015).

Smoothing procedures of satellite image time-series help to grasp a clear picture of trends and patterns in the time-series data. In this study, a combination of moving average and lowess filter (locally weighted regression) were employed to capture the long-term profile and trends of mean, SD, minimum and maximum NDVI over the years. Moving average filter is described as the simplest form of *Savitsky-Golay filter* and helps to reduce disturbances in the image (Jonsson & Eklundh 2004). The lowess smoothing filter is one of the nonparametric fitting techniques and does not require prior assumption on the relationship between dependent and independent variables. It renders a graphic summary of relationships between variables (Cleveland 1979; Jacoby 2000). The success of the lowess smoothing highly depends on the smoothing parameter ($\alpha$, ranges between 0 and 1) which helps to specify the proportion of observations to be considered in the local regression. The default α value in lowess smoothing is 0.65 considering 65% of the data for estimating the weights in the local regression (Jacoby, 2000).

### 3.2.3. Rainfall Data and Analysis

Monthly total rainfall and temperature (monthly maximum and minimum) covering a period of 16 years (2000-2015) was obtained from two meteorological stations in Addis Ababa. These stations are Bole (2354 meters above sea level) and Addis Ababa (2386 meters above sea level).

Missing monthly rainfall (8% for Bole station and 5.7% for Addis Ababa station) and temperature (7% for Bole station and 0.5% for Addis Ababa station) data was normalized by replacing them with the long-term monthly averages of the same month to make the analysis more meaningful.

The rainfall data obtained from the two stations was only at monthly total level. On the other hand, mean, SD, maximum, and minimum NDVI values were extracted from MODIS at image level. Therefore; Aggregated annual maximum and annual mean rainfall values were standardized to Z-score to make the comparison easier using the following formula.

$$Zr = \frac{(Rr - Mr)}{SDr} \qquad \text{Eq. 3}$$

*Where;*

*Zr= standardized maximum rainfall for each year*

*Rr= recorded maximum rainfall value for each year (n=12);*

*Mr = mean value of rainfall in that year (n =12)*

*SDr = standard deviation of rainfall in the same year (n = 12).*

To standardize maximum and mean NDVI values in the same scale, the same formula was applied. Since the DN values were obtained at image level (n = 387), the average of the yearly maximum NDVI value was aggregated and used for analysis.

$$Zn = \frac{(AMx - Mx)}{SDx} \qquad \text{Eq. 4}$$

*Where;*

*Zn = standardized yearly maximum NDVI*

*AMx= yearly maximum NDVI DN values (n=23);*

*Mx = yearly mean NDVI DN value of that year (n = 23)*

*SDx = SD of NDVI DN values in the same year (n =23).*

# Chapter Four: Results and Discussion

## Introduction

This chapter presents the results of the study in three separate, but interrelated sections. Section 4.1 covers LULC change which is generated using LANDSAT 7 ETM$^+$ and LANDSAT 8 (OLI). Section 4.2 presents trends of greenness in the study area based on NDVI which is derived from the processing and analysis of MODIS data. Mean, SD (standard deviations), maximum and minimum values of NDVI are used to discuss trends over a period of 17 years. The detailed image processing procedures for extracting information is described in chapter three of this thesis. Section 4.3 deals with the integration of NDVI with Meteorological based rainfall data. Each sections are followed by discussion of the results referring to literatures and findings of other similar studies.

## 4.1. Land Use Land Cover Change in Addis Ababa and its Surrounding

Four thematic land cover classes (Built-up, vegetation, agriculture and water) were identified using supervised classification (with maximum likelihood algorithm) (Figure 4.1; Figure 4.2). The classification of the 2000 Landsat ETM$^+$ is carried out with an *overall accuracy* of 83% and *Kappa coefficient* of 76% (Appendix 1). The *overall classification accuracy* and *kappa statistics* of the 2017 Landsat 8 (OLI) image were 90% and 86% respectively (Appendix 2). The discussion in this section focused on land cover classes which have shown significant change: Built-up (any artificial surface including buildings, roads, concrete and so on) vegetation (woodlands and trees either natural or plantations) and agriculture (land used for cultivating crops including grazing land).

Land use and land cover (LULC) change detection result has shown that the *change no-change* classes were found to be 427(35%) and 790 (65%) sq km respectively. The study revealed a decrease in agricultural land by 285 sq km (34%). The built up area has increased by 357 sq km (183%) between 2000 and 2017 in the study area (Figure 4.2).

Decline in agricultural land is mainly in response to population pressure which ignited massive demand on land mainly for housing and other infrastructural developments which were seen in the city.

As reported by Azeb (n.d.), the city of Addis Ababa has witnessed housing deficit since the 1970s. In 1994, the number of housing units was 374,742, which is 9.5% less than the total number of households. By 2004, however; the difference increased to 24.8%, regardless of an increase in housing units to 471,429. Though there is lack of exact statistical figures on land demand, Yusuf, Tefera & Zerihun (2009) estimated that Addis Ababa needs additional 5-600,000 housing units given its rapid population growth and persistent gap between housing demand and supply.

Between 1996 and 2006, for example; the city government of Addis Ababa has delivered 12,063 plots covering 4.1 sq km of land to residents including apartments. The average annual number of plots allotted for residents were 1,100 with an area of 0.4 sq km (Ysuf, Tefera & Zerihun 2009). This was, however; a negligible attempt to address the demand for housing. As a result, the government introduced other programs and projects. One of these projects was the *integrated housing development* *program* (IHDP) which was partly aimed to increase the housing supply and thereby reduce sub-standard houses. UN_HABITAT (2011) has noted that the IHDP was successful in building 171,000 out of 400,000 housing units targeted between 2005 and 2010. Accordingly, about 20 sq km of land has been transformed to condominium housing in all sub cities of Addis Ababa since the initiation of IHDP in 2005 (AACAILIC 2015). Despite, IHDP was successful in reducing slums and producing sizeable number of housing units, it did not last long as an alternative option, especially to the poor.

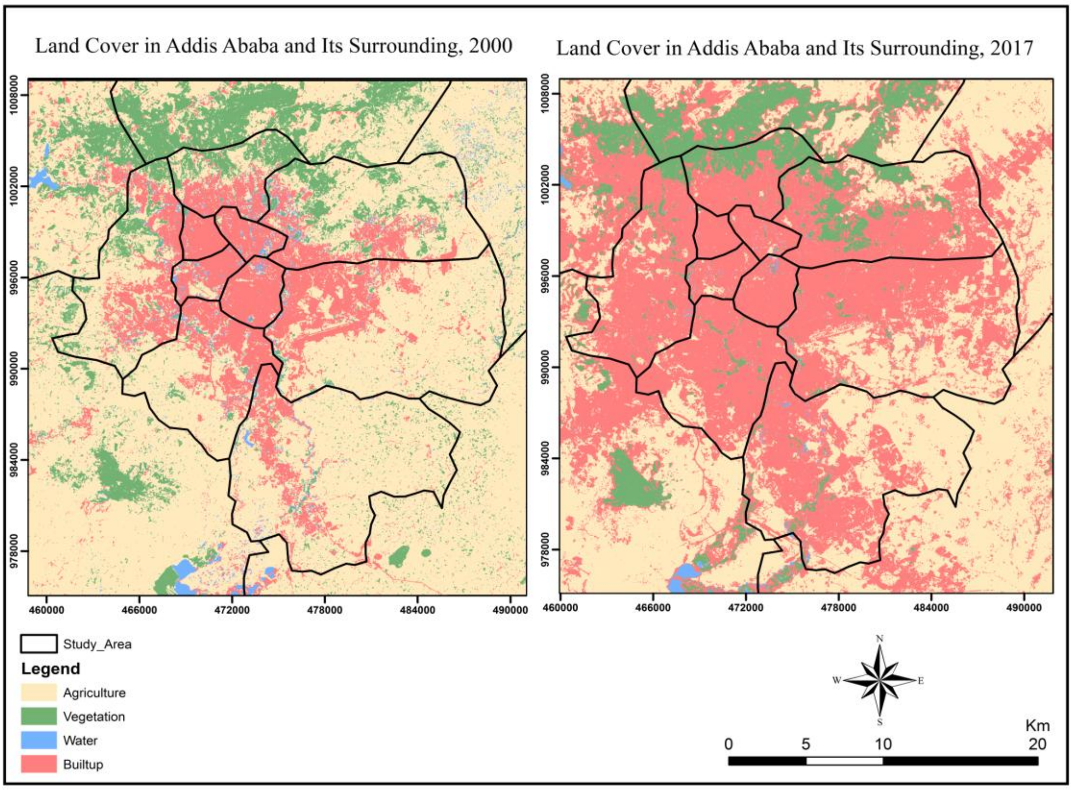


*Figure 4.1. Land cover classification map of LANDSAT 7 ETM+ and LANDSAT 8 (OLI)*

Besides, illegal settlements have been equally expanding claiming sizeable portion of agricultural land. The informal sector (illegal settlement) supplies about 35% of the housing supply between 1996 and 2003 in Addis Ababa (UN_HABITAT 2011). This scenario seems continuing in response to government's failure to address the demand for land/housing at affordable prices.

Similarly, there has been a general rise in the number of certificates offered for real estate developers from 33 in 1994 to 1,734 in 2001 and to 2,328 in 2006 (Ysuf, Tefera & Zerihun 2009). Presently, there are about 6000 real estate developers who are in the waiting list to obtain land for investment (Berihu, Alebel &. Weldeselasie 2017).

Furthermore, introducing railway line, new roads, new housing areas and urban utilities greatly demand land. Since recent years, LULC change in the main agricultural lands surrounding Addis Ababa has become a very sensitive issue in the politics and continued to be a point of debate and conflict. This is partly, because the expansion is at the expense of the livelihood of farmers surrounding the metropolitan city, Addis Ababa.

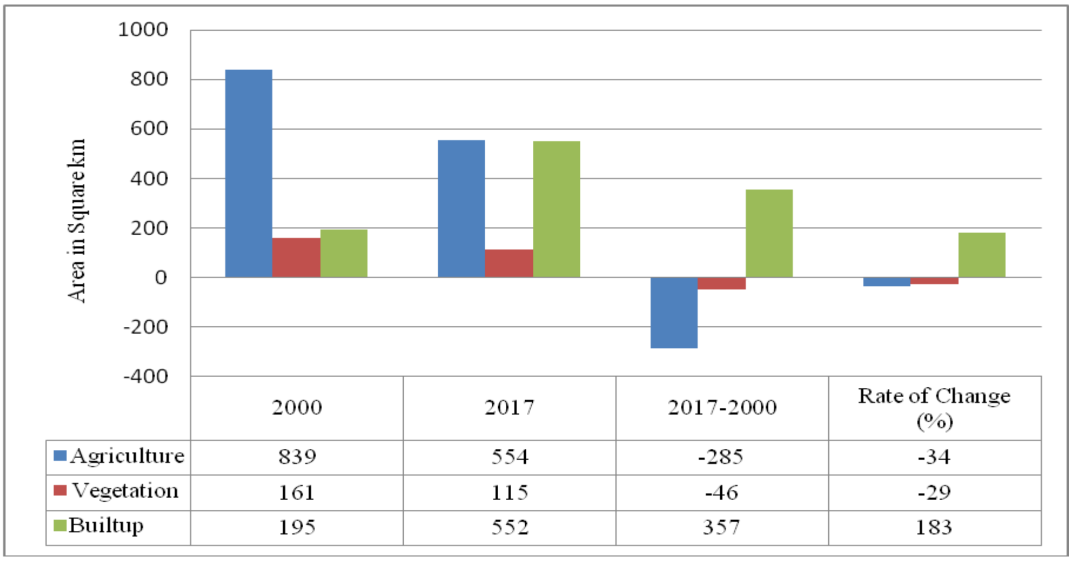


*Figure 4.2. LULC change in Addis Ababa and its surrounding (2000-2017)*

As shown in Figure 4.2, vegetation cover is reduced by 29% between 2000 and 2017 in the study area. This is mainly explained by the expansion of agricultural land (7%) (this is negligible and happens when farmers feel short of land for agriculture) and built-up areas (12%) (Table 4.1). Encroachment in to agricultural land and illegal cutting of trees was reported by Shikur (2011) in Addis Ababa. The same study estimated over 10,500 women who are engaged in wood collection for their livelihoods.

*Table 4.1. Major Land Cover Change Classes (2000-2017)*

| Land Cover Change | Area in Square km | Percent |
|---|---|---|
| Agriculture to Vegetation | 30 | 7 |
| Agriculture to Built-up | 317 | 74 |
| Vegetation to Agriculture | 31 | 7 |
| Vegetation to Built-up | 49 | 12 |
| Total | 427 | 100 |

*Source: LANDSAT 7 ETM$^{+}$ and LANDSAT 8 (OLI) supervised classification*

Albeit there is a net-loss in vegetation, the current study has revealed that there is LULC conversion from agriculture to vegetation (30 sq km) as shown in Table 4.1 and Figure 4.3. This implies the action taken by the government to relocate some farmer households who were living inside the protected area called *Entoto*. This is a good practice to increase vegetation cover, species diversity and adjust the local climate.

The establishment of *Gulele Botanical Garden* (GBG) is a notable achievement to safeguard destruction of forests and increase the species diversity and maintain the local climate in the northern part of Addis Ababa. The GBG was established in 2005 covering a total area of 7.05 sq km. Currently, it is home to more than 240 plant species of which more than 30 are endemic. According to the information from the

GBG, the institution started field-level recording of phenological characteristics of species and this is important for cross-validation of remote sensing results with the reality in the future.

A land cover change study by Fetene and Worku (2013) in the upper catchment of Addis Ababa using LANDSAT TM/ETM 1986, 2000 and 2011 has revealed 6% increase in overall forest coverage. However, the study only considered the Northern part of Addis Ababa which is relatively restrictive for the expansion of built-up areas and habitat destruction. Conversely, the current study attempts to monitor land cover change at larger extent, Addis Ababa and its surrounding. Applying different classification techniques, it was revealed that built surface has increased by 338% in Addis Ababa between 1985 and 2010. The same study revealed a declining trend in vegetation (Feyisa et al. 2016). This result is comparable with the findings of the current study though there is a slight difference in the spatial extent of the study area.

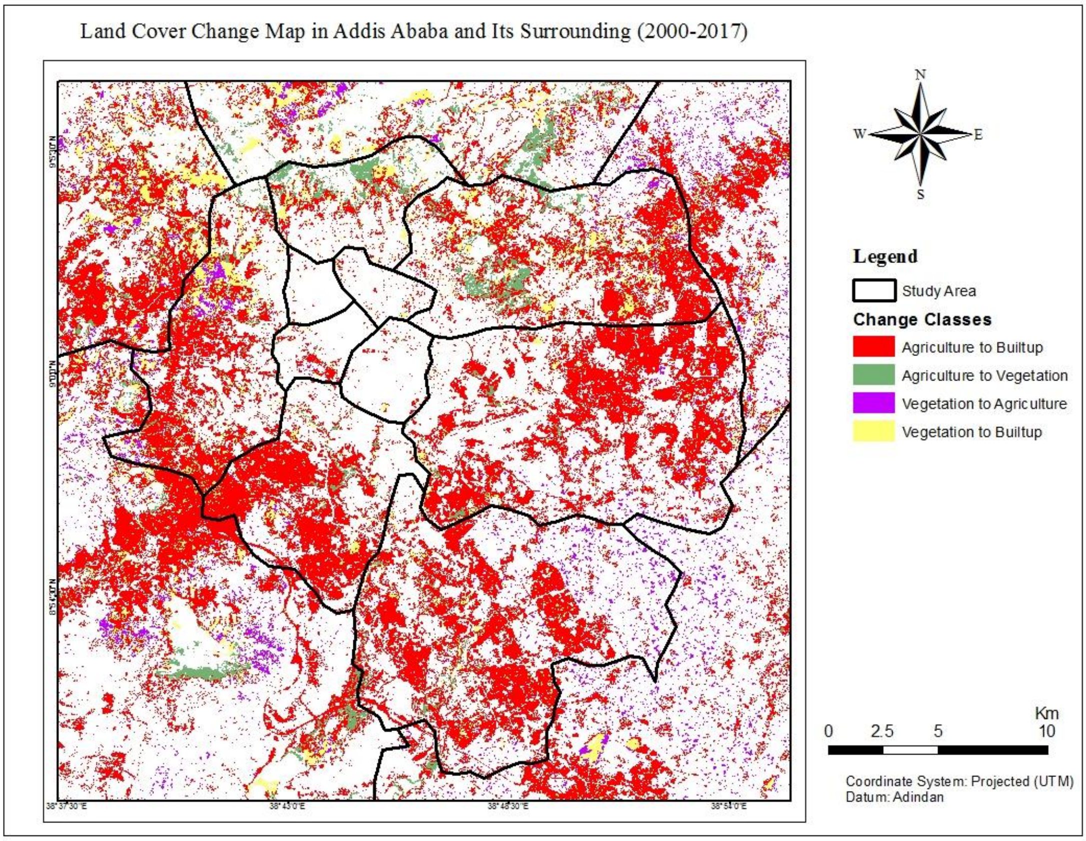


*Figure 4.3. Land cover change map in Addis Ababa and its surrounding (2000-2017)*

Using aerial photos of 2006 and 2011, a land cover change study by Tekle (2016) revealed substantial reduction of agricultural land by 24%. Vegetation was found to be increased by 0.8%. The study reported that the built-up area has increased from 48% in 2006 to 58% in 2011. The current study revealed an increase of built-up area from 17% to 45% and a decrease of agricultural land from 70% to 45% between 2000 and 2017. The disparity seen is due to difference in time and the spatial extent of study area. The slight increase in vegetation cover of Addis Ababa reported (mainly in the upper catchment) might be related to the rehabilitation programs carried out by stakeholders including the GBG.

The preceding paragraphs reveal substantial conversion former agricultural and vegetation land to built-up area (86%) between 2000 and 2017. Climate is adversely impacted by land conversions, especially; with disproportionate expansion of built-up areas at the expense of vegetation cover and agricultural land. Among others, an increase in urban heat intensity is reported by other studies as discussed in section 4.2.

## 4.2. Trends of Greenness in Addis Ababa and its Surrounding (2000-2016)

### 4.2.1. Trends and Temporal Variability in NDVI

Figure 4.4, illustrates that there are some noisy pixels in the time-series data. To reduce random noise and clearly see the seasonal trends and variability in NDVI, the time-series was decomposed using additive decomposition method (Appendix 3) and then smoothed using a *moving average* (Figure 4.4) *and lowess* (Figure 4.6) smoothing filter.

The trends of NDVI vary greatly across the time-series years. For example; the mean NDVI values drop between 2002 and 2004, rise in 2005 and 2007 and decline in 2009, 2013 and 2016. The linear and non-linear trends of mean, maximum and SD NDVI time series shows a generally declining trend (Appendix 3 and Appendix 4).

To further understand NDVI profile, the yearly mean values of NDVI were plotted separately per image acquisition dates (Figure 4.5). The yearly mean NDVI profile shows that Addis Ababa and its surrounding experiences *bi-modal NDVI periods*.

The *first NDVI period* is characterized by very narrow peak and base. To make the description less complex, years which have a relatively similar mean annual NDVI curves were grouped together. The *first group of mean NDVI years* are (2001, 2004, 2006 and 2007). For this years, onset of the *first NDVI period* starts in early to mid January ($1^{st}$ or $17^{th}$) and peaks in late February ($49^{th}$) day of the year and *senescence* abruptly after the same date. The *second group* (2000, 2003, 2005, 2010) reveal a relatively wider base. Nevertheless, there is considerable difference in the *onset* and *senescence* dates of this group. For the *third group* (2011, 2012, 2013), the *onset* is on the $33^{rd}$ or $49^{th}$ and the peak is on the $65^{th}$ or $81^{st}$ day of the year which is March. *Group four* (2002, 2014, 2015, 2016) start the onset on $1^{st}$ January and peak on the $113^{th}$ day of the year, which is April. The year 2002, however; peaks on the $81^{st}$ day. This group of years are still different, because; the $1^{st}$ NDVI peak period has a wider peak and base compared to the second NDVI period. *Group 5* (2008 and 2009) were found to be unique having a similar *onset* and slight difference in their *peak* and *senescence* days.

The *second NDVI period* has a relatively wider peak and base covering a couple of months. The *first category* constitutes the majority of the years (2000, 2001, 2004, 2005, 2006, 2007, 2010, 2011, 2012) and start their *onset* between $97^{th}$ (early April) to $129^{th}$ day of the year (early May). For this category of years, NDVI mostly peaks between $177^{th}$ (late June) and $209^{th}$ (late July) days of the year. The peak continues until the $241^{st}$ day of the year which is late August and starts to decline afterwards. The end dates (dormancy) vary greatly across years but it mostly falls on (or after) the $273^{rd}$ day of the year which is the end of September. The *second category* (2003, 2008, 2009) have a relatively unique and varied time series. They start the second NDVI period on the $157^{th}$ date, experience a relatively narrow peak and a sudden senescence (2002, 2008). NDVI peak varies to this group but falls either earlier in May (2002) or late in September (2003). The *peak* and *senescence* days for the years 2008 and 2009 is found to be similar with the majority of the time-series years. The *third category* (2014, 2015, 2016) reveal a surprising NDVI time-series with a highly variable NDVI peaks and minimum DN values compared to other categories.

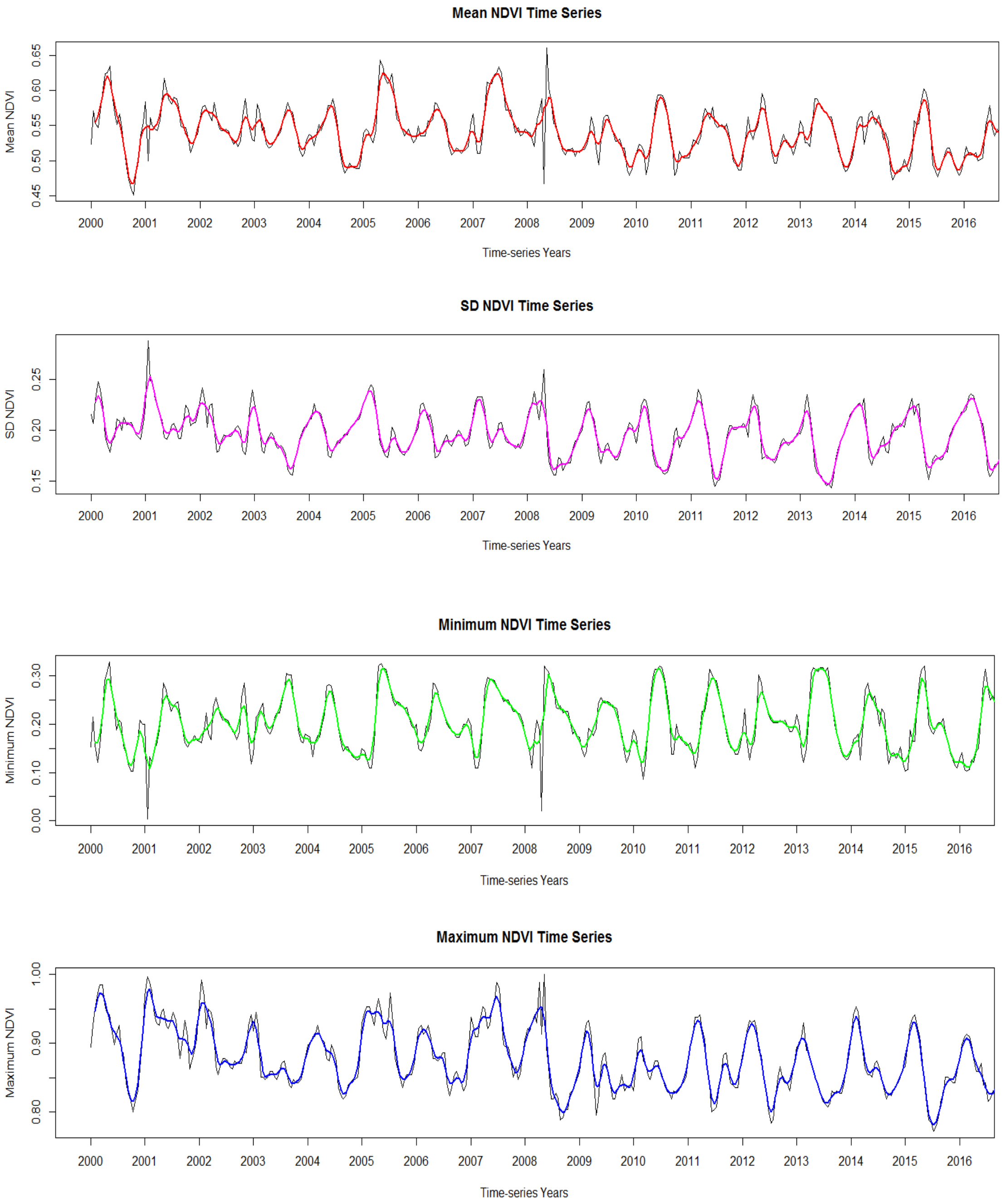


*Figure 4. 4. MODIS based NDVI time-series in Addis Ababa using Moving average filter*

Two alpha values (α = 0.65 and α = 0.33) of the lowess were used to smooth the mean, maximum, minimum and SD NDVI values and capture the trend over the years (Figure 4.6). The result reveals a clear decreasing trend in the mean, maximum and SD NDVI values over the years. The minimum NDVI vales seem to have a different trend: increased sharply (2000-2005), remained stable (2006-2010) and declined after 2010 making the range to be decreasing over the time-series years. From figure 4.6 it can be understood that the value (α = 0.33) better fits NDVI trend over the years. The default lowess smoothing alpha value ($\alpha = 0.65$) over-smoothed the data and does not help to capture variation between the time series years. Generally; declining trends of mean, maximum, minimum and SD in NDVI imply a net-loss in greenness in the study area over the time-series years.

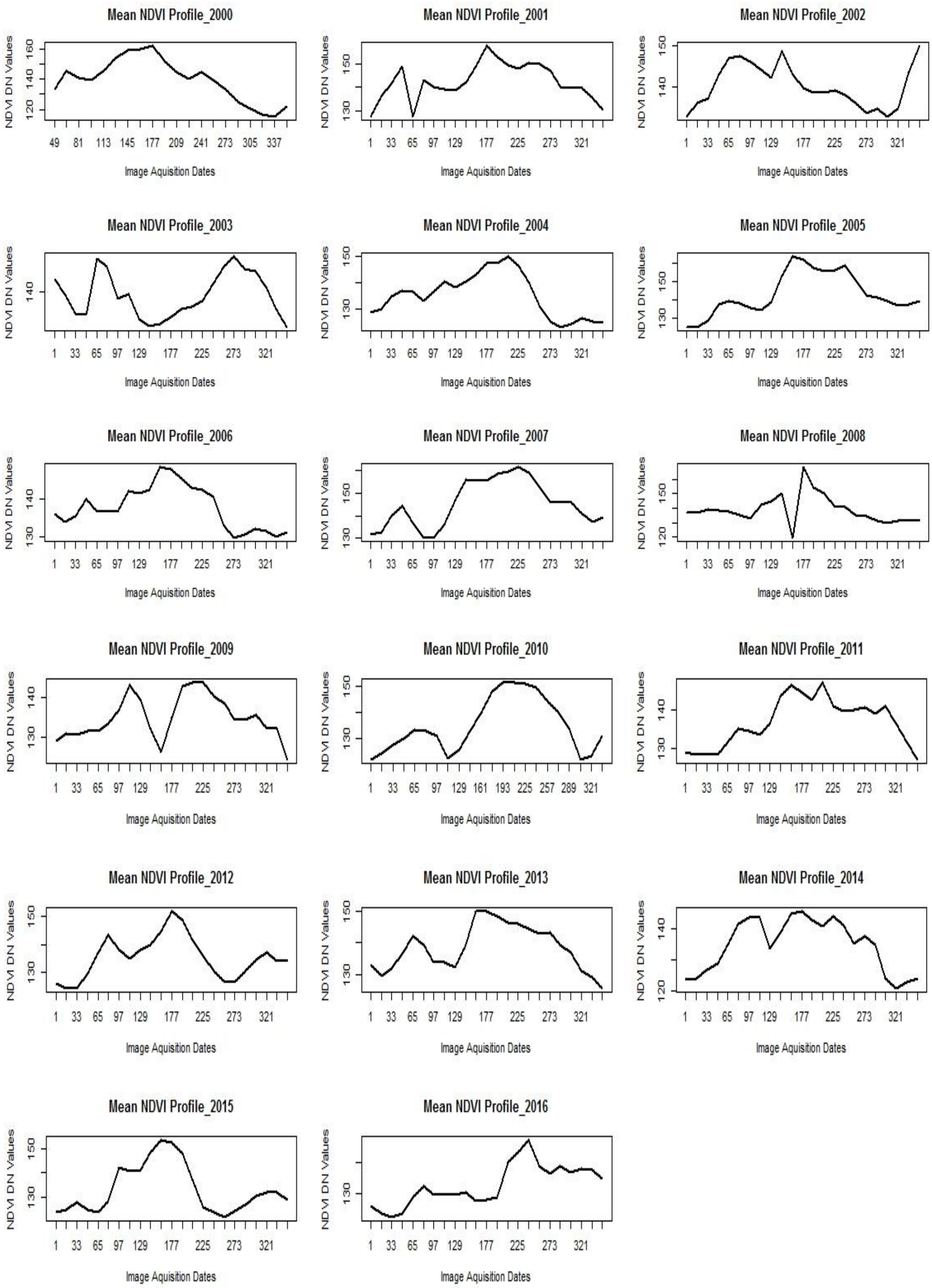


*Figure 4.5. MODIS based annual mean NDVI profile per image acquisition dates (2000-2016)*

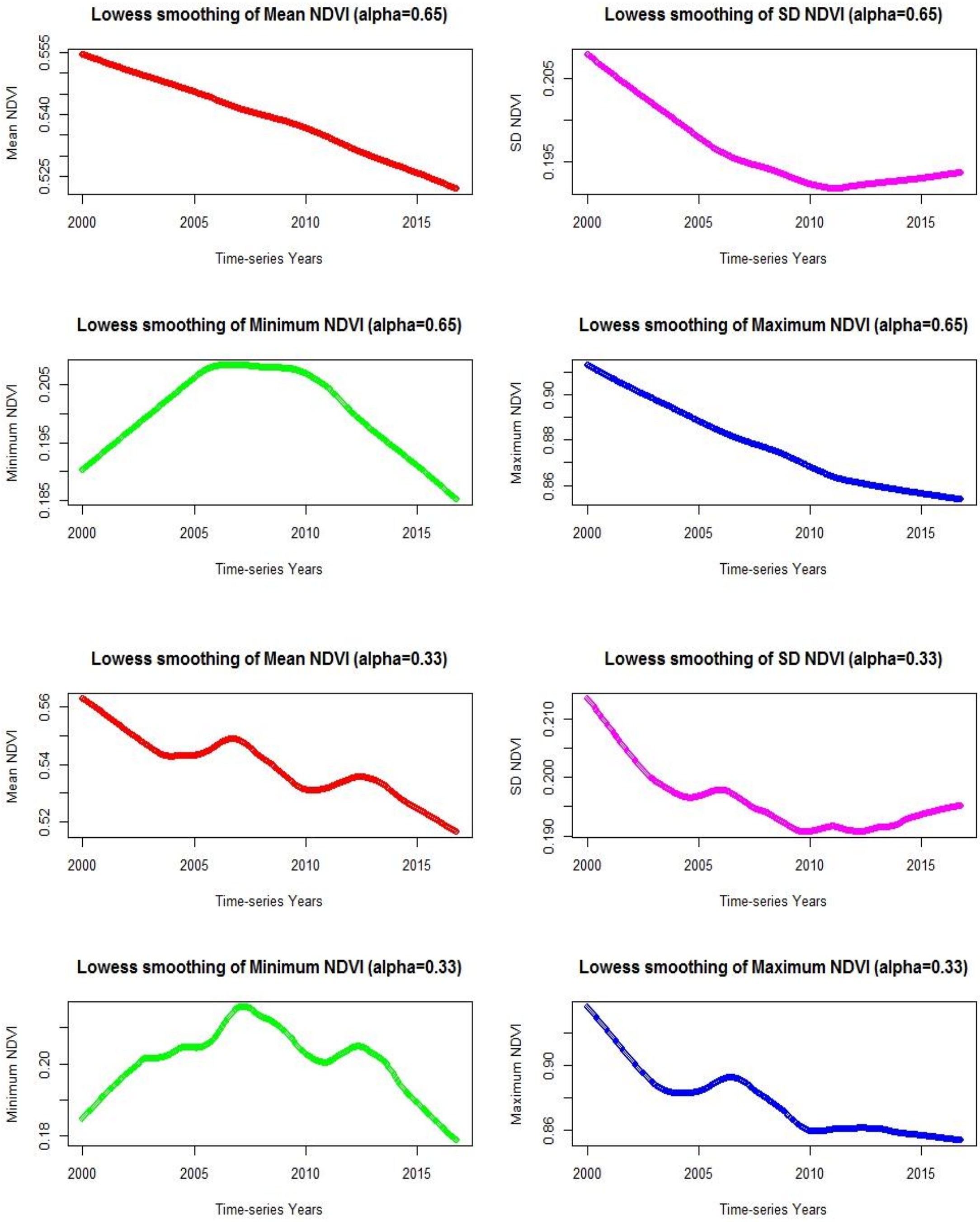


*Figure 4. 6. MODIS based linear trends of NDVI in Addis Ababa using Lowess-filter*

### 4.2.2. Spatial Variation in NDVI and its Link with LULC Change

This study was partly aimed to analyze the spatial variation of NDVI time-series in the study area. Accordingly, the aggregated mean, SD, maximum and minimum NDVI values were visualized (Figure 4.7) to examine spatial variation in greenness over the time-series years under consideration.

The mean map illustrates that pixels with very minimum DN values are predominantly distributed in the central, southern, south-eastern and western pars of Addis Ababa. Decrease in NDVI time-series trend discussed in the previous section seems to happen in these areas. The intensity still vary with in these areas, for example; western and south-western parts have low intensity of mean NDVI indicating a relatively higher greenness. Pixels with maximum mean values are predominantly seen in the northern and north-western part of the study area. The land cover classification result in section 4.1 has shown that these areas are found to be more vegetated (Figure 4.1). This has an implication on the spatial variation in the intensity and direction of LULC change and rapid urbanization in the study area.

Based on spatial variability maps (mean, SD, maximum, and minimum) the study area can be classified in to three NDVI zones: *the central zone* with very low SD pixels, the *transitional zone* with medium SD pixels and the *periphery* with higher SD pixels.

There is high variation in DN values along the peripheral areas as opposed to the main urban area. Low SD pixels at the center implies little or no variability in greenness in these areas due to homogenous built-up area dominating the center. There is still a clear contrast between pixels within the central zone. The SD pixels with low DN values seem contagious mainly occupying the central parts of Addis Ababa and expanding to the transitional zones. Nevertheless, the variability maps reveal that pixels with low DN values show a leapfrogging tendency in the north-western and south-western parts of the study area. This might be due to land conversions in these areas.

The *transitional zone* between the city and its surrounding experience medium contrast in greenness. This implies that these areas have a mixed LULC (vegetation, agriculture plus built-up) compared to the center and the peripheral zones. Nevertheless, there is a tendency that land conversions is negatively impacting greenness in these areas over time.

The *periphery* is characterized by pixels with high SD values. Higher SD implies that the periphery exhibits a comparatively more vegetation and agriculture than built-up areas.

The aggregated minimum NDVI pixels, reveal a similar spatial pattern in NDVI pixels like the mean ensuring low greenness in the central and southern part, high greenness in the northern part and a relatively better greenness in the western and north-western part of the study area.

The aggregated maximum NDVI values map identifies the main urban center, Addis Ababa, with very low DN values. Very high intensity of greenness is seen in the urban fringe where there are relatively higher coverage of vegetation. Pixels with agricultural crops (especially during the production season) also have a similar spectral reflectance like vegetation and this impact is clearly seen in the aggregate maximum NDVI map being distributed in different corners of the study area.

The preceding paragraphs have shown MODIS based NDVI trends and spatial variability of greenness in Addis Ababa and its surrounding over a period of 17 years (2000-2016). The results have revealed that there is a trend of NDVI decline predominantly in the eastern and southern and slightly in the western parts of the study area. This implies net-loss in greenness in these areas over time. Considerable spatial variations were seen in the mean, SD, maximum and minimum NDVI trends as well.

The question is, what are the responsible factors for the fall in greenness in the study area: natural or anthropogenic? The main natural/physical factors might be variability and reduction in rainfall induced by climate change over time. Anthropogenic factors are connected with rapid urbanization, decline in vegetation cover and agricultural land due to human intervention. Farmers cropping calendar, due to rainfall variability would greatly impact NDVI trends as well.

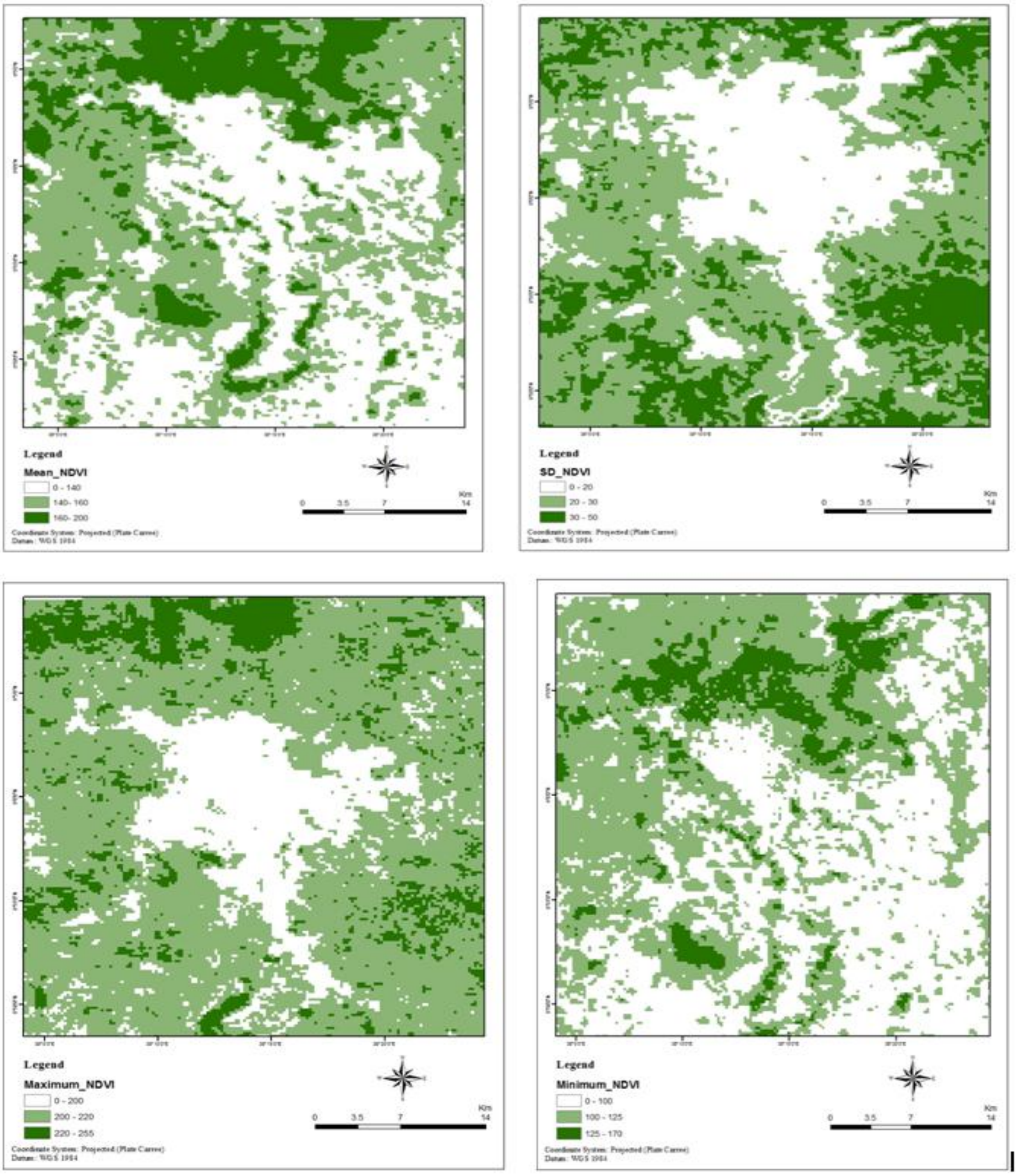


*Figure 4.7. MODIS based spatial configuration of NDVI in the study area (2000-2017)*

The change detection result discussed in section 4.1 revealed rapid urbanization at the expense of vegetation cover and agricultural land. As can be seen from Figure 4.1 and Figure 4.2, the change classes are spatially located in the *NDVI transitional zones* and slightly *in the peripheral zones* discussed in the current section. In the same fashion, decrease in mean, maximum and SD DN values implies that the study area has been becoming homogenous due to land conversions, particularly; increased urbanization at the expense of vegetation cover and agriculture. Therefore; land conversion can be taken as an evidence for the decline in NDVI trends over the time series years (2000-2016) in Addis Ababa and its surrounding.

A study on land degradation and regeneration in Mongolia revealed that MODIS based positive and negative NDVI trends mostly coincided with areas of land cover change implying an increase or a decrease in vegetation, respectively (Eckert et al. 2015). MODIS land surface temperature (LST) data was linked to phenological transition dates in mid and high latitudes. The study revealed notable delays in the onset of green-up and dormancy in urban areas due to urban heat island effects and the mean annual urban temperature was found to be 1-3$^{\circ}$C higher relative to its surrounding (Zhang et al. 2004).

Studies have revealed the adverse impacts of rapid urbanization on the green cover explained by NDVI and land surface temperature (LST) (Sharma & Joshi 2016; Son et al. 2017; Singh et al. 2017; Yang et al. 2017; Chen et al. 2017). Another study by Feyisa et al. (2016) revealed the thermal effect of rapid urbanization and has shown that heat intensity decreases with distance from the center to the periphery between 1985 and 2010.

Field based temperature data (Appendix 7) shows that the mean annual temperature is increasing over the time-series in the study area. Nevertheless; considering many stations and their spatial configuration covering the rural and urban setting would provide a good insight regarding variation in heat intensity. This issue seems interesting for further research by integrating field based and satellite based data.

Agricultural practices in tropical areas are often integrated with trees or tree crops which are important to balance the local climate. Studies reveal that trees outside forests (be it on agricultural land or on the streets), small parks and urban forests have a positive impact to regulate the local climate (Horst 2006).

An investigation on the efficiency of parks in reducing urban warming was studied by (Feyisa, Dons, & Meilby, 2014). The study revealed that the parks cooling intensity (PCI) is positively related to NDVI derived from LANDSAT ETM thermal band. The same study has concluded that cooling effect highly depends on the type of species, cover of the canopy, the shape and size of the parks. An interesting finding by the same study was that the cooling effect of eucalyptus tree was high. Conversely, there seems a campaign to reduce the coverage of this species from most areas of Addis Ababa due to its adverse impact on soil fertility and water content (Horst 2006). The impact of trees outside forests and their contribution to local climate also seems interesting for further research.

Therefore; attention should be given by urban planners and ecologists to integrate greening activities with urbanization, because; helps to exploit the multifaceted advantages of urban vegetation and greening: regulation of local climate, aesthetic values, educational and scientific values. Land should be given attention and monitored properly by the government to ensure its optimal use by balancing the demand of many stakeholders: residents, farmers, real estate developers, NGOs, companies and so on. The role of remote sensing and GIS applications for monitoring is pivotal and should be promoted.

## 4.3. Integrating MODIS Based NDVI with Station Based Rainfall Data

In this section of the paper, emphasis has been given to understand the trends of rainfall distribution based on field data obtained from two stations, namely; Bole and Addis Ababa. Attempt was made to discuss whether meteorological based rainfall data is related to MODIS based NDVI trends discussed in section 4.2.

The trends of mean, maximum and SD of rainfall and NDVI is illustrated in Figure 4.8. Rainfall variability is clearly observable over the years. The mean rainfall trend in both stations reveals a general decline since 2010/2011. However, NDVI decline started earlier in 2008/2009. Years like 2001, 2005 and 2007 received a relatively higher mean annual rainfall. This is again seen on the aggregated maximum rainfall and NDVI curves. The maximum values of rainfall and NDVI started to decline after 2011/12.

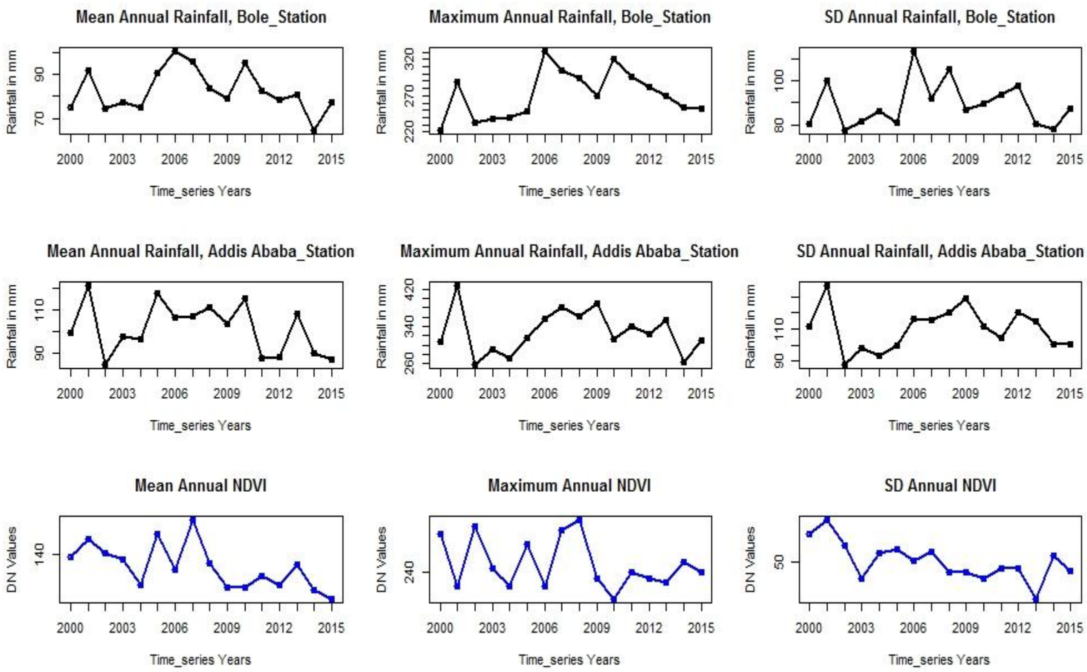


*Figure 4.8. Comparison of MODIS based NDVI time-series with station based rainfall (2000-2015)*

Figure 4.9 illustrates standardized annual maximum rainfall in the two stations in comparison with NDVI. The maximum rainfall recorded at Bole station reveal a slightly increasing trend compared to Addis Ababa station. However, maximum NDVI has shown a declining trend. Compared to NDVI, maximum rainfall seems stable in the study area. This implies that NDVI is also influenced by other variables. NDVI values are positively correlated with the rainfall data obtained from the two stations (Figure 4.11 and Appendix 8).

As can be seen from Figure 4.10, the aggregated annual mean NDVI and rainfall shows a declining trend, especially; after 2008/2009. The correlation coefficient between standardized mean NDVI and rainfall was tested (Figure 4.9). The result shows that Addis Ababa station has a better correlation with ($R^2 = 0.25$). Bole station revealed ($R^2 = 0.2$) (at 95% confidence level). The slight disparity in $R^2$ is partly explained by elevation difference in the two stations. This value calls for considering explanatory variables other than rainfall for further research.

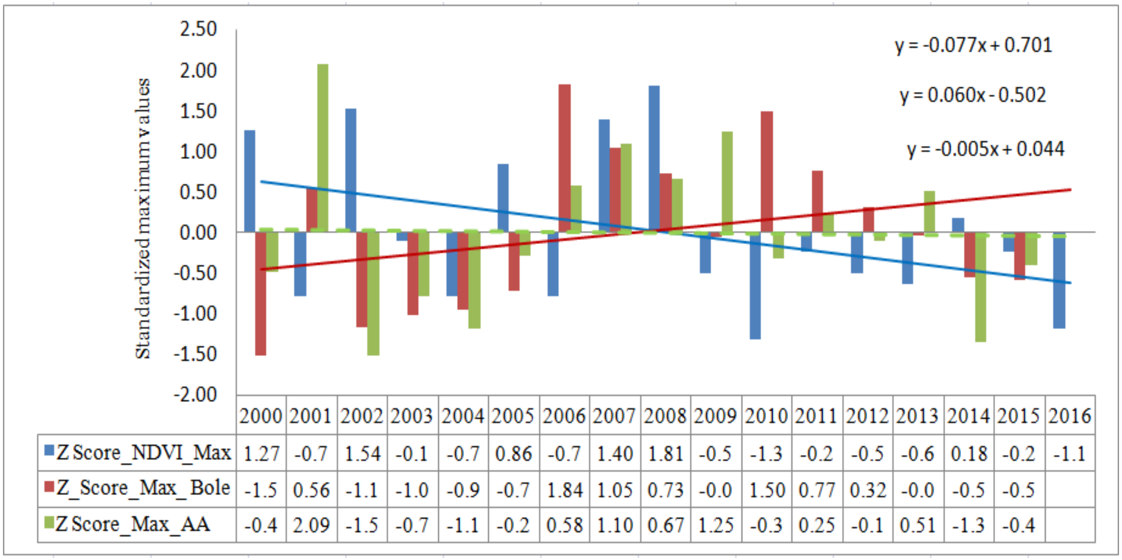


| | 2000 | 2001 | 2002 | 2003 | 2004 | 2005 | 2006 | 2007 | 2008 | 2009 | 2010 | 2011 | 2012 | 2013 | 2014 | 2015 | 2016 |
|---|---|---|---|---|---|---|---|---|---|---|---|---|---|---|---|---|---|
| Z Score_NDVI_Max | 1.27 | -0.7 | 1.54 | -0.1 | -0.7 | 0.86 | -0.7 | 1.40 | 1.81 | -0.5 | -1.3 | -0.2 | -0.5 | -0.6 | 0.18 | -0.2 | -1.1 |
| Z_Score_Max_Bole | -1.5 | 0.56 | -1.1 | -1.0 | -0.9 | -0.7 | 1.84 | 1.05 | 0.73 | -0.0 | 1.50 | 0.77 | 0.32 | -0.0 | -0.5 | -0.5 | |
| Z Score_Max_AA | -0.4 | 2.09 | -1.5 | -0.7 | -1.1 | -0.2 | 0.58 | 1.10 | 0.67 | 1.25 | -0.3 | 0.25 | -0.1 | 0.51 | -1.3 | -0.4 | |

*Figure 4.9. Aggregated annual maximum NDVI and rainfall (standardized)*

If the study had considered many rainfall stations which were selected based on averaged image pixels, the correlation coefficient result would be different. Nevertheless, a study has shown that rainfall data obtained from a climatic station is roughly valid for areas which are found within a radius of 20 kilometers (Seboka, 2016). Based on the analysis of AVHRR GIMMS data for a period between 1982 and 2006, the correlation between rainfall and NDVI in Addis Ababa was found to be positive ($R^2$= 0.23). This finding coincides with the current study ($R^2$ = 0.25 for Addis Ababa station and $R^2$ = 0.2 for Bole station). The same study revealed that NDVI trends is found to be strongly correlated with rainfall and at climate stations level and decreases afterwards (Seboka 2016). Another study by Eckert et al. (2015) has shown that precipitation changes in the same time period seem to have had an influence on large NDVI trend areas.

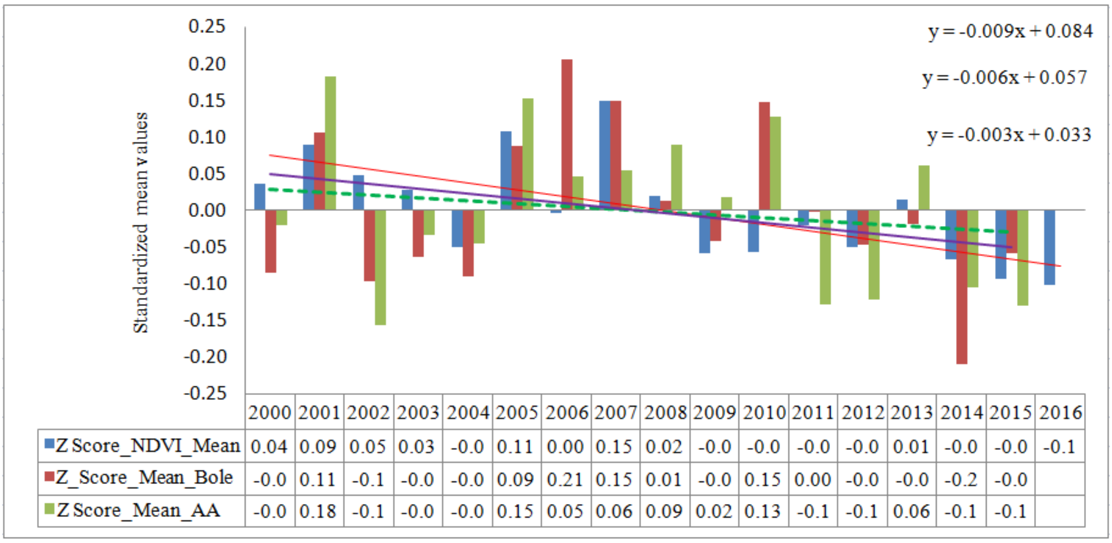


| | 2000 | 2001 | 2002 | 2003 | 2004 | 2005 | 2006 | 2007 | 2008 | 2009 | 2010 | 2011 | 2012 | 2013 | 2014 | 2015 | 2016 |
|---|---|---|---|---|---|---|---|---|---|---|---|---|---|---|---|---|---|
| Z Score_NDVI_Mean | 0.04 | 0.09 | 0.05 | 0.03 | -0.0 | 0.11 | 0.00 | 0.15 | 0.02 | -0.0 | -0.0 | -0.0 | -0.0 | 0.01 | -0.0 | -0.0 | -0.1 |
| Z_Score_Mean_Bole | -0.0 | 0.11 | -0.1 | -0.0 | -0.0 | 0.09 | 0.21 | 0.15 | 0.01 | -0.0 | 0.15 | 0.00 | -0.0 | -0.0 | -0.2 | -0.0 | |
| Z Score_Mean_AA | -0.0 | 0.18 | -0.1 | -0.0 | -0.0 | 0.15 | 0.05 | 0.06 | 0.09 | 0.02 | 0.13 | -0.1 | -0.1 | 0.06 | -0.1 | -0.1 | |

*Figure 4.10. Aggregated annual mean NDVI and rainfall (standardized)*

The preceding paragraphs have shown that rainfall and NDVI trends are comparable in many ways with notable disparities. For example, the aggregated NDVI and rainfall time-series reveals that NDVI trend declined earlier (2008/2009) though rainfall in both stations started to decline in 2010/2011. NDVI declines faster compared to rainfall as shown in Figure 4.9 and 4.10.

NDVI is sensitive to various factors: soil moisture content, the onset and offset of agricultural season (farmers cropping calendar), rainfall variability, seasonality, LULC change and so on. In the current study, however; correlation between NDVI and rainfall was tested only considering the rainy season.

Ethiopia experiences four seasons, namely; *Kiremt* (June, July, August), *Bega* (December, January, February), *Belg* (March, April and May), and *Tsedey* (September, October and December). These seasons are equated with *summer, winter, spring* and *autumn* respectively. To make the discussion on trends of mean and maximum NDVI and rainfall more meaningful and comparable, the months of the year receiving maximum rainfall (May, June, July, August and September) and image acquisition dates covering these months were take in to account. Actually, maximum value composite (MVC) MODIS images are provided with dates starting from 1$^{st}$ of January to 353$^{th}$ day of the year which falls in December. Therefore, MODIS Images and their NDVI values covering 129$^{th}$ to 273$^{th}$ days of the year were considered for rainy season analysis.

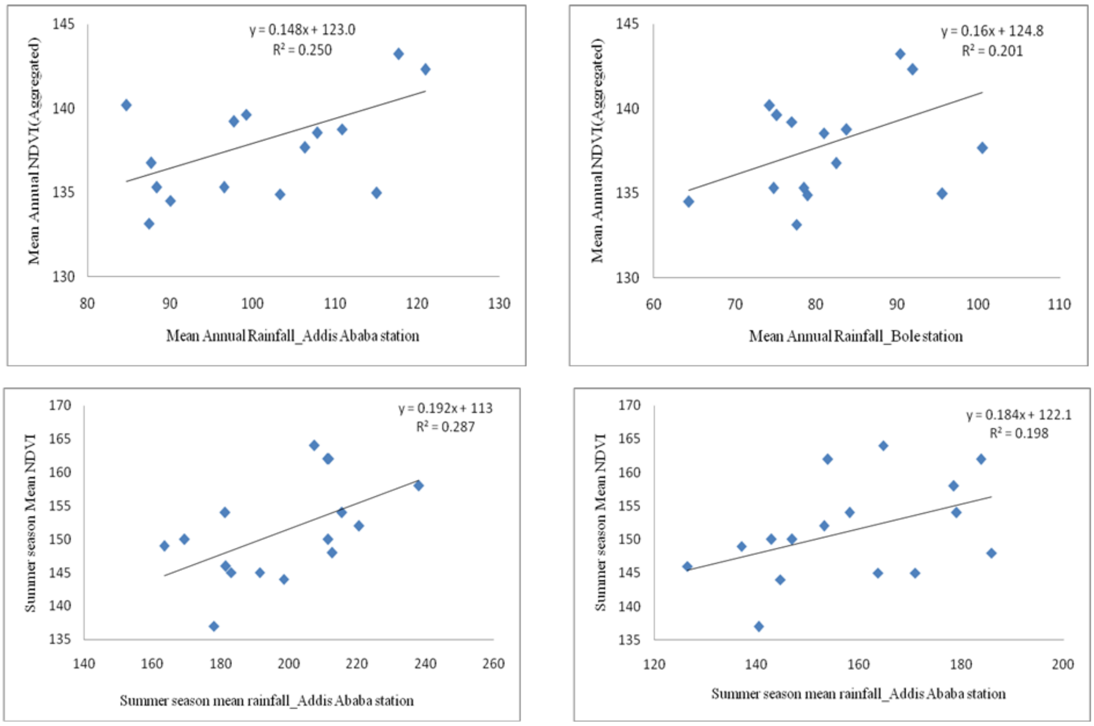


*Figure 4.11. Correlation between mean NDVI and rainfall (2000-2015)*

The result reveals that there is a slight improvement in the correlation coefficient between mean NDVI and rainfall for Addis Ababa station with a value of ($R^2$ = 0.29). The coefficient value for Bole station remained the same at ($R^2$ = 0.2) (Figure 4.11). Years like 2001, 2005 and 2007 have received a relatively higher rainfall over the years (Figure 4.9, 4.10, and 4.12). The correlation coefficient between the maximum NDVI and rainfall is shown in (Figure 4.12 and Appendix 8 ). Higher $R^2$ values between NDVI and rainfall were revealed for higher rainfall years (2001, 2005 and 2007) implying the role of rainfall in NDVI. Nevertheless; the yearly correlation result between maximum rainfall and NDVI shows a decreasing trend over the years (Figure 4.12).

The yearly rainfall trends of Addis Ababa and Bole station are presented in appendix 5 and 6 respectively. NDVI trends discussed in section 4.2 and the yearly rainfall data obtained from field measurements are comparable in many ways. It was discussed that MODIS based time-series curves are characterized by bi-modal NDVI peaks representing two seasons experienced by the study area: the first season is with narrow peak and base representing a very short NDVI period. The second season exhibits a wider peak and base representing the longest rainy season in the study area covering a couple of months. In the same fashion, the yearly trends of rainfall in the two stations reveal that Addis Ababa and its surrounding receives bi-modal rainfall. Similar to NDVI, the first and short rainfall season peaks either in March or April. The onset of the main rainy season mostly falls in April or May. The rainfall mostly peaks in July and August and then declines in September.

The foregoing paragraphs have shown that MODIS based NDVI trends and station based rainfall data are positively related with lower $R^2$ values. The correlation coefficient between NDVI and rainfall discussed in the previous section might be highly influenced by the mixed nature of LULC (vegetation, agriculture and built-up) in the study area. Provided that the study area was homogenous, the relationship between NDVI and rainfall would be different. Therefore; studying a purely urban area separated from agriculture and vegetated surfaces will provide a different result. Ultimately, consideration of other variables which are not explained in the current research is recommended for further study.

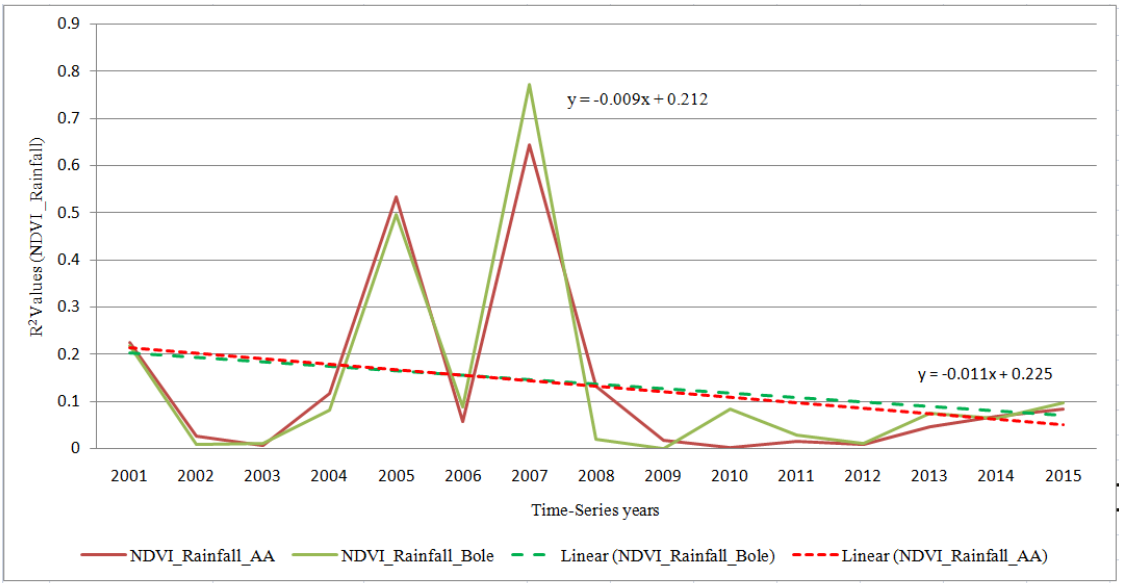


*Figure 4.12. Trends of annual maximum NDVI and Rainfall ($R^2$ values) over the years*

# Chapter Five: Conclusions

The study was carried out in Addis Ababa and its surrounding covering 1,217 sq km. The research questions raised were: *1) What does the trends of greenness and its spatio-temporal variability look like? 2) What are the major LULC change classes in the study area and how are they related to NDVI trends? and 3) Does field based rainfall and satellite based NDVI correlate?.*

LULC change detection has shown that the *change no-change* classes were found to be 427(35%) and 790 (65%) sq km respectively. The study revealed a net-loss in agricultural land by 285 sq km (34%) and vegetation by 46 sq km (29%). Conversely, the built up area has increased by 357 sq km (183%) between 2000 and 2017 in the study area. The majority of Addis Ababa and its surrounding (86%) was converted to built-up area.

A general decline in trends of NDVI implying net-loss in greenness was revealed in the study area. Considerable spatial variation were shown in the mean, SD, maximum and minimum NDVI trends. Decrease in the mean, maximum and SD NDVI implies that the study area has been becoming homogenous due to land conversions, particularly of increased urbanization, at the expense of vegetation cover and agriculture which is negatively impacting greenness over the years.

Spatially, three classes of NDVI were identified: *low NDVI zone* (the center with homogeneous built-up area); *medium NDVI zone* (the transitional zone with mixed LULC) and *high NDVI zone* (the periphery with a relatively higher vegetation cover). LULC change classes were found to be predominantly located in the *NDVI transitional zones* and slightly in the *peripheral zones*.

MODIS based NDVI revealed a bi-modal NDVI trend in the study area and this result is found to be similar with station based rainfall seasons. The onset, green-up (peak), senescence, and end dates of NDVI and rainfall seasons were found to be comparable in many ways with notable disparities. For example, NDVI started to decline earlier (2008/2009) than rainfall in the time-series (2010/11). The disparity being revealed between rainfall and NDVI seem to be explained by other variables which are not the subject of the current study.

NDVI is found to be moderately correlated with aggregated mean rainfall data ($R^2$ = 0.25 Addis Ababa station; $R^2$ = 0.2 Bole station). The correlation result between maximum rainfall and NDVI revealed a decreasing trend over the years (declined highly after 2010). Years like 2001, 2005 and 2007 have shown higher $R^2$ values. The correlation seems to be highly reduced by the influence of LULC change (reduction in agriculture and vegetation) than decline in rainfall.

Considering a homogenously vegetated and/or agricultural area separated from a highly mixed urban area might yield a different correlation coefficient between NDVI and rainfall. Factors like irrigation, soil moisture content, farmers cropping calendar due to rainfall variability also influence NDVI. These factors need to be considered for further research.

Ultimately, the role of remote sensing and GIS applications for monitoring is pivotal and should be promoted.

## References

AACA (Addis Ababa City Administration). 2009. Addis Ababa population images. Population affairs coordination sub process, Finance and economic development bureau. Report, Addis Ababa, 52 pp [English]

AACAILIC (Addis Ababa City Administration Integrated Land Information Center ). 2007. Addis Ababa City Atlas (1st ed). Report, Addis Ababa, 190 pp [English].

Adole, T., Dash, J. & Atkinson, P.M. 2016. A systematic review of vegetation phenology in Africa. *Ecological Informatics*, 34,117–128. DOI:10.1016/j.ecoinf.2016.05.004.

Azeb Kelemework Bihon. (nd). Housing for the Poor in Addis Ababa. Report, Addis Ababa, 17 pp [English].

Berihu assefa gebrehiwot, alebel b. Weldeselasie, M. G. 2017. Growing demand, shrinking supply of industrial lands in addis ababa, ethiopia: underlying causes and possible solutions. Paper prepared for presentation at the 2017 world bank conference on land and poverty the world bank - Washington DC, march 20-24, 2 (pp. 1–17).

Claudia K, Stefan D, and W.W. 2015. Remote Sensing Time Series : Revealing Land Surface Dynamics: Status Quo and the Pathway Ahead. In K. Claudia, D. Stefan, & W. Wagner, eds. 1-24 pp. Switzerland: Springer International Publishing.

Cleveland, W. S. 1979. Robust Locally Weighted Regression and Smoothing Scatterplots. *Journal of the American Statistical Association*, 74: 829–836.

Chen, Y., Chiu, H., Su, Y., Wu, Y., & Cheng, K. 2017. Landscape and Urban Planning: Does urbanization increase diurnal land surface temperature variation ? Evidence and implications. *Landscape and Urban Planning*, 157, 247–258. DOI: 10.1016/j.landurbplan.2016.06.014

Daniels, P. W. 2004. Urban challenges: The formal and informal economies in mega-cities. *Cities*, 21, 501–511. DOI:10.1016/j.cities.2004.08.002

Dell, M., 2009. GIS Analysis for Applied Economists, Prepared for Programming for Economists. Department of Economics, Massachusetts Institute of Technology. Report, Massachusttes, 48 pp [English]

De Paul, O. V. 2007. Remote sensing: New applications for urban areas. *Proceedings of the IEEE*, 95, 2267–2268. DOI:10.1109/JPROC.2007.908065

Elias, Y. 2008. Revisiting “Slums”, Revealing Responses: Urban upgrading in Tenant-dominated Inner-City Settlements, in Addis Ababa, Ethiopia. PhD Thesis, Trondheim, Norway, NTNU

Eckert, S., Hüsler, F., Liniger, H., & Hodel, E. 2015. Trend analysis of MODIS NDVI time series for detecting land degradation and regeneration in

Mongolia. *Journal of Arid Environments*, 113,16–28.

Fetene, A., & Worku, H. 2013. Planning for the conservation and sustainable use of urban forestry in Addis Ababa, Ethiopia. *Urban Forestry and Urban Greening*, 12, 367–379. DOI:10.1016/j.ufug.2013.03.004

Feyisa, G.L., Dons, K. & Meilby, H. 2014. Efficiency of parks in mitigating urban heat island effect: An example from Addis Ababa. *Landscape and Urban Planning*, 123, 87–95.

Feyisa, G. L., Meilby, H., Darrel Jenerette, G., & Pauliet, S. 2016. Locally optimized separability enhancement indices for urban land cover mapping: Exploring thermal environmental consequences of rapid urbanization in Addis Ababa, Ethiopia. *Remote Sensing of Environment*, 175, 14–31. DOI:10.1016/j.rse.2015.12.026

Gebeyehu Admasu, T. 2015. Urban land use dynamics, the nexus between land use pattern and its challenges: The case of Hawassa city, Southern Ethiopia. *Land Use Policy*, *45*, 159–175. DOI:10.1016/j.landusepol.2015.01.022

Horst, A. 2006. Rehabilitation of urban forests in Addis Ababa Rehabilitation of Urban Forests in Addis Ababa. *Journal of the Drylands* 1, 108- 117.

Huete, A., Didan, K., Miura, T., Rodriguez, E. P., Gao, X., & Ferreira, L. G. 2002. Overview of the radiometric and biophysical performance of the MODIS vegetation indices. *Remote Sensing of Environment*, *83*, 195–213. DOI: 10.1016/S0034-4257(02)00096-2

Huete, A. Miura, T. Yoshioka, H. Ratana, P. & Broich, M. 2014. Indices of Vegetation Activity . In J. M. Hanes, eds. 1-41 pp. Heidelberg: Springer International Publishing.

Huete, A. 2014. Vegetation Indices. In E. G. Njoku, ed. pp. 1689–1699. New York. Springer Science and Business Media

Jacoby, W. G. 2000. Loess : a nonparametric graphical tool for depicting relationships between variables . *Electoral Studies*, 19, 577–613.

Jensen, R., J. 2000. *Remote sensing of the environment: an earth resource perspective* (2nd ed). Prentice-Hall, Inc

Jin, H. & Eklundh, L. 2014. A physically based vegetation index for improved monitoring of plant phenology. *Remote Sensing of Environment*, 152, 512–525. DOI: 10.1016/j.rse.2014.07.010.

Jones, G., H., & Vaughan, A., R. 2010. *Remote sensing of vegetation: principles, techniques and applications*. USA, Oxford University Press.

Jonsson P & Eklundh L. 2004. TIMESAT — a program for analyzing time-series of satellite sensor data. *Computers & Geosciences*, 30, 833–845. DOI:10.1016/j.cageo.2004.05.006

Kong, Y., Meng, Y., Li, W., Yue, A., & Yuan, Y. 2015. Satellite Image Time Series Decomposition Based on EEMD. *Remote Sensing*, 7, 15583–15604.

DOI: 10.3390/rs71115583

Li, F., Han, L., Liujun, Z., Yinyou, H., & Song, G. 2016. Urban Vegetation Mapping Based on the Hj-1 Ndvi Reconstrction. *ISPRS - International Archives of the Photogrammetry, Remote Sensing and Spatial Information Sciences*, *XLI-B8*, 867–871. DOI:10.5194/isprsarchives-XLI-B8-867-2016

Lillesand, T., M., Kiefer, R., W., & & Chipman, J., W. 2015. *Remote sensing and image interpretation* (7th ed). USA: John Wiley &Sons Inc.

Lu, D., Mausel, P., BrondÃ-zio, E., & Moran, E. 2009. Change detection techniques. *International Journal of Remote Sensing*, 25, 2365–2401. DOI:10.1080/0143116031000139863

NMA (National Meteorology Agency). Retrieved 10 November, 2016 from. http://www.ethiomet.gov.et/climates/climate_of_city/3352/Addis Ababa.

Pettorelli1, N., Vik1, J, O., Mysterud1,A., Gaillard, J, M., Tucker, C, J., & Stenseth, N, C. 2005. Using the satellite-derived NDVI to assess ecological responses to environmental change. *Trends in Ecology and Evolution*, 20, 503–510.

Prema, V., & Rao, K. U. 2015. Time series decomposition model for accurate wind speed forecast. *Renewables: Wind, Water, and Solar*, 2, 1–11. DOI:10.1186/s40807-015-0018-9

Rouse, J. W.1974. Monitoring the vernal advancement and retrogradation (greenwareeffect) of natural vegetation. Greenbelt, MD, USA, NASA/GSFCT, Type 3, Final Report

Seboka, G.N. 2016. Spatial Assessment of NDVI as an Indicator of Desertification in Ethiopia using Remote Sensing and GIS. Master Thesis. Lund, Sweden: Lund University

Schneider, A., Friedl, M. A., & Potere, D. 2010. Mapping global urban areas using MODIS 500-m data: New methods and datasets based on urban ecoregions. *Remote Sensing of Environment*, *114*, 1733–1746. DOI: 10.1016/j.rse.2010.03.003

Sharma, R., & Joshi, P. K. 2016. Urban Climate Mapping: environmental impacts of rapid urbanization in the National Capital Region of India using remote sensing inputs. *Urban Climate*, 15, 70–82. DOI:10.1016/j.uclim.2016.01.004

Shikur, E.T. 2011. Challenges and problems of urban forest development in Addis Ababa , Ethiopia. *Trees, people and the built environment*: *Proceedings of the Urban trees research conference*, No.017 pp.130-140. Birmingham, UK, 13-14 April 2011.

Singh, P., Kikon, N., & Verma, P. 2017. Impact of land use change and urbanization on urban heat island in Lucknow city , Central India . A remote sensing based estimate. *Sustainable Cities and Society*, 32, 100–114. DOI: 10.1016/j.scs.2017.02.018

Sivakumar, V. 2014. Urban Mapping and Growth Prediction using Remote

Sensing and GIS Techniques, Pune, India. *ISPRS - International Archives of the Photogrammetry, Remote Sensing and Spatial Information Sciences*, XL-8-2014.

Son, N., Chen, C., Chen, C., & Thanh, B. 2017. Assessment of urbanization and urban heat islands in Ho Chi Minh City , Vietnam using Landsat data. *Sustainable Cities and Society*, 30, 150–161. DOI:10.1016/j.scs.2017.01.009

Suepa, T., Qi, J., Lawawirojwong, S., & Messina, J. P. 2016. Understanding spatio-temporal variation of vegetation phenology and rainfall seasonality in the monsoon Southeast Asia. *Environmental Research*, *147*, 621–629. DOI:10.1016/j.envres.2016.02.005

Tadesse, T., Berhan, G., Zaitchik, B., & Dinku, T. 2014. Satellite-based hybrid droughtmonitoring tool for prediction of vegetation condition in Eastern Africa: A case study for Ethiopia. *Water Resources Research*, 2176–2190. DOI: 10.1002/2013WR014281.Received

Teferi, E., Uhlenbrook, S., & Bewket, W. 2015. Inter-annual and seasonal trends of vegetation condition in the Upper Blue Nile (Abay) Basin: Dual-scale time series analysis. *Earth System Dynamics*, *6*, 617–636. DOI:10.5194/esd-6-617-2015

Tekle Woldegerima Kahsay. 2016. Study of the Urban Environment and Ecosystem Services of Addis Ababa : Implications for Urban Greenspace Planning . PhD Thesis, Addis Ababa: Addis Ababa university

Tolon, U., W. 2008. Comparison of urban upgrading projects on development corporation in Ethiopia. Report, 56 pp [English]. Reterived on 10 November 2016, from. https://upcommons.upc.edu/handle/2099.1/637

UN-HABITAT. 2011. Condominium Housing in Ethiopia: The Integrated Housing Development Programme. Retrieved 15 November 2016, from. http://www.iut.nu/Facts and figures/Africa/Ethiopia_CondominiumHousingUN-Habitat2011.pdf

UN (United Nations). 2014. World Urbanization Prospects. Department of Economic and Social Affairs. Retrieved 15 November 2016, from http://esa.un.org/unpd/wup/Highlights/WUP2014-Highlights.pdf

UN (United Nations). 2016. The Sustainable Development Goals Report 2016, 56. Retrieved 15 November 2016, from. http://doi.org/10.7202/051028ar

Westinga, E. 2004. Manual of land cover mapping and monitoring . Enschede, ITC, The Netherlands

Wubneh, M. 2013. Addis Ababa, Ethiopia – Africa's diplomatic capital. *Cities*, 35, 255–269. DOI:10.1016/j.cities.2013.08.002

Xuanlong, M., Huete, A., Yu, Q., Davies, K., & Coupe, N. R. 2012. Monitoring Spatial Patterns of Vegetation Phenology in an Australian Tropical Transect Using MODIS EVI. *International Archives of Photogrammetry, Remote Sensing and Spatial Information Sciences XXXIX*, 271–276.

Yang, J., Sun, J., Ge, Q., & Li, X. 2017. Urban Forestry & Urban Greening Assessing the impacts of urbanization-associated green space on urban land surface temperature : A case study of Dalian , China. *Urban Forestry & Urban Greening*, 22, 1–10. DOI:10.1016/j.ufug.2017.01.002

Yengoh, G. T., Dent, D., Olsson, L., & Tengberg, A. E. 2015. Use of the Normalized Diff erence Vegetation Index (NDVI) to Assess Land Degradation at Multiple Scales: Current Status, Future Trends, and Practical Considerations. Heidelberg, New York, Dordrecht, and London. Springer Cham

Yirgalem, M. 2009. Manipulating Ambiguous Rules: Informal Actors in Urban land Management, a Case Study in Kolfe-Keranio Sub-city, Addis Ababa. *Proceedings of the 16th International Conference of Ethiopian Studies*, *I*, 929–942. Trondheim, Norway.

Yusuf, B; Tefera, S, Zerihun, A. 2009. Land Lease Policy in Addis Ababa. Addis Ababa chamber of commerce and sectoral associations. Addis Ababa, Ethiopia. Report, 140 pp [English]. Addis Ababa Chamber of Commerce

Xie, Y., Sha, Z. & Yu, M., 2008. Remote sensing imagery in vegetation mapping: a review. *Journal of Plant Ecology*, 1, 9–23.

Yuan, F., Sawaya, K. E., Loeffelholz, B. C., & Bauer, M. E. 2005. Land cover classification and change analysis of the Twin Cities (Minnesota) metropolitan area by multitemporal LANDSAT remote sensing. *Remote Sensing of Environment*, *98*, 317–328. DOI:10.1016/j.rse.2005.08.006

Zhang, X., Friedl, M. A., Schaaf, C. B., Strahler, A. H., Hodges, J. C. F., Gao, F., … Huete, A. 2003. Monitoring vegetation phenology using MODIS. *Remote Sensing of Environment*, *84*, 471–475. DOI:10.1016/S0034-4257(02)00135-9

Zhang, X., Friedl, M., A., Schaaf, C., B., & Strahler, A., H. 2004. Climate controls on vegetation phenological patterns in northern mid- and high latitudes inferred from MODIS data. *Global Change Biology*, 10,1133–1145.

Zhu, Z., Fu, Y., Woodcock, C. E., Olofsson, P., Vogelmann, J. E., Holden, C., … Yu, Y. 2015. Including land cover change in analysis of greenness trends using all available LANDSAT 5, 7, and 8 images: A case study from Guangzhou, China (2000-2014). *Remote Sensing of Environment*, *185*, 243–257. DOI:10.1016/j.rse.2016.03.036

# Appendixes

***Appendix 1**. Accuracy Report_2000*

CLASSIFICATION ACCURACY ASSESSMENT REPORT

Image File : e:/2000_again_supervised.img
User Name : Tesfaye
Date : Wed Apr 12 15:20:28 2017

ACCURACY TOTALS

| Class Name | Reference Totals | Classified Totals | Number Correct | Producers Accuracy | Users Accuracy |
|---|---|---|---|---|---|
| Unclassified | 0 | 0 | 0 | --- | --- |
| Agriculture | 87 | 88 | 74 | 85.06% | 84.09% |
| Water | 35 | 31 | 27 | 77.14% | 87.10% |
| Vegetation | 45 | 55 | 41 | 91.11% | 74.55% |
| Built-up | 41 | 34 | 30 | 73.17% | 88.24% |
| Totals | 208 | 208 | 172 | | |

Overall Classification Accuracy = 82.69%

----- End of Accuracy Totals -----

KAPPA (K^) STATISTICS

Overall Kappa Statistics = 0.7557
Conditional Kappa for each Category.

| Class Name | Kappa |
|---|---|
| Unclassified | 0.0000 |
| Agriculture | 0.7265 |
| Water | 0.8449 |
| Vegetation | 0.6752 |
| Built-up | 0.8535 |

----- End of Kappa Statistics -----

***Appendix 2***. *Accuracy Report_2017*

CLASSIFICATION ACCURACY ASSESSMENT REPORT
-----------------------------------------

Image File : e:/2017_again_supervised.img
User Name : Tesfaye
Date : Wed Apr 12 17:44:12 2017

ACCURACY TOTALS
----------------

| Class Name | Reference Totals | Classified Totals | Number Correct | Producers Accuracy | Users Accuracy |
|---|---|---|---|---|---|
| Agriculture | 66 | 82 | 66 | 100.00% | 80.49% |
| Vegetation | 62 | 55 | 54 | 87.10% | 98.18% |
| Water | 40 | 37 | 37 | 92.50% | 100.00% |
| Built-up | 70 | 64 | 56 | 80.00% | 87.50% |
| Totals | 238 | 238 | 213 | | |

Overall Classification Accuracy = 89.50%

----- End of Accuracy Totals -----

KAPPA (K^) STATISTICS
---------------------

Overall Kappa Statistics = 0.8579

Conditional Kappa for each Category.
------------------------------------

| Class Name | Kappa |
|---|---|
| Agriculture | 0.7300 |
| Vegetation | 0.9754 |
| Water | 1.0000 |
| Builtup | 0.8229 |

----- End of Kappa Statistics -----

***Appendix 3***. *An example of mean additive decomposition for separating random noise and seasonality from the non-linear trend.*

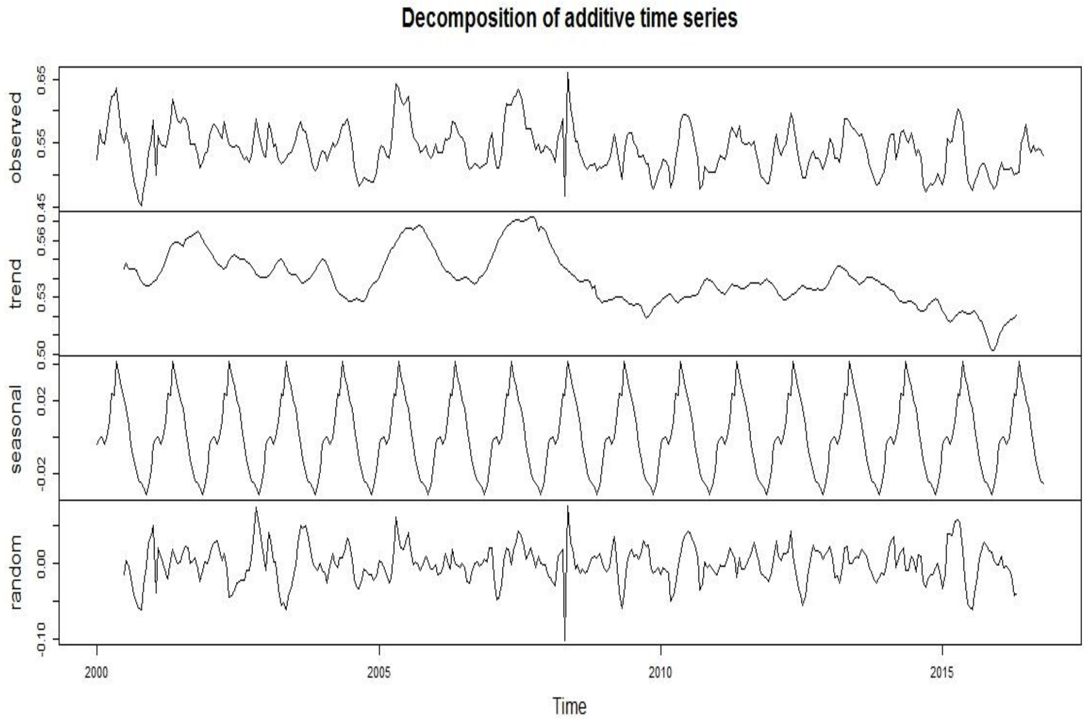


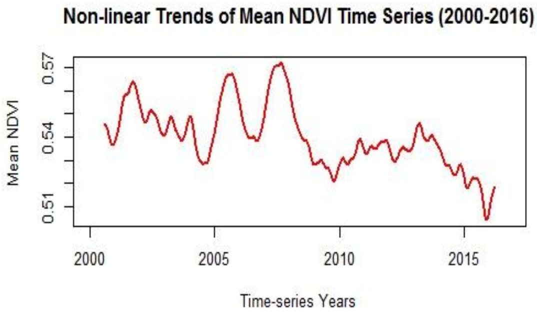


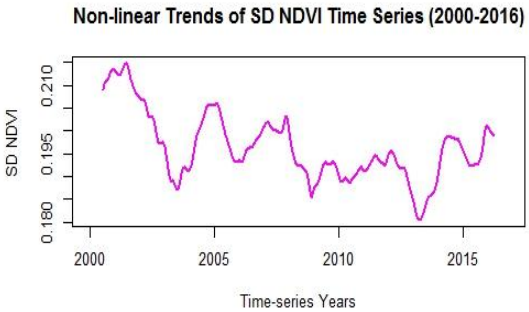


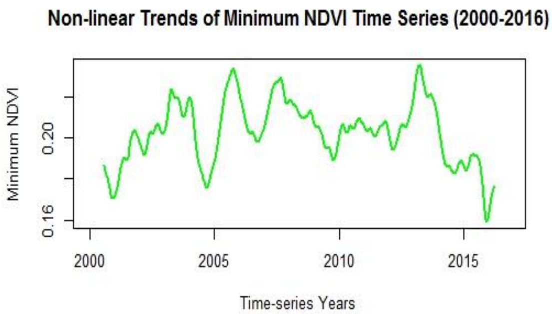


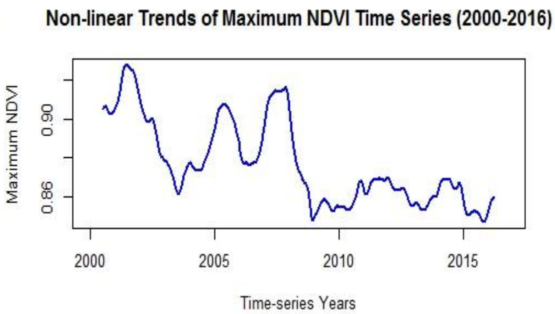

*__Appendix 4__. Linear trends of  NDVI time-series per image acquisition dates*

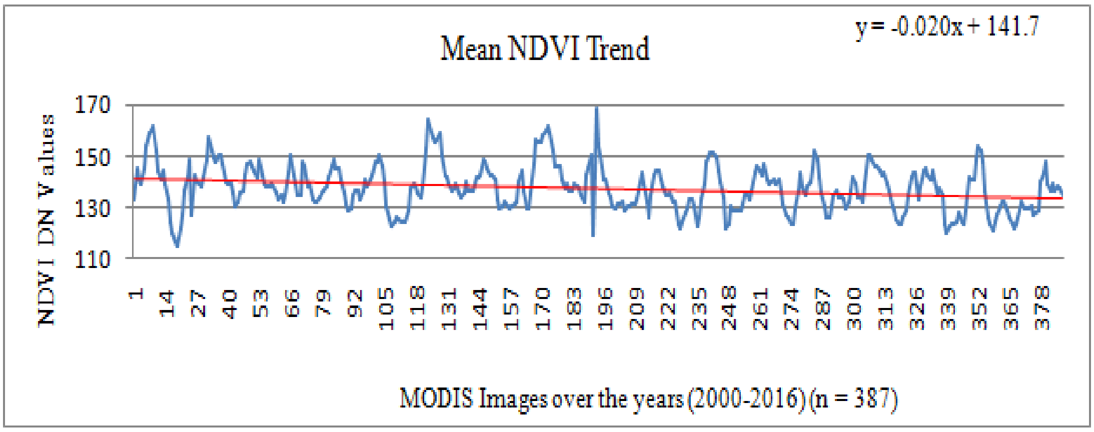


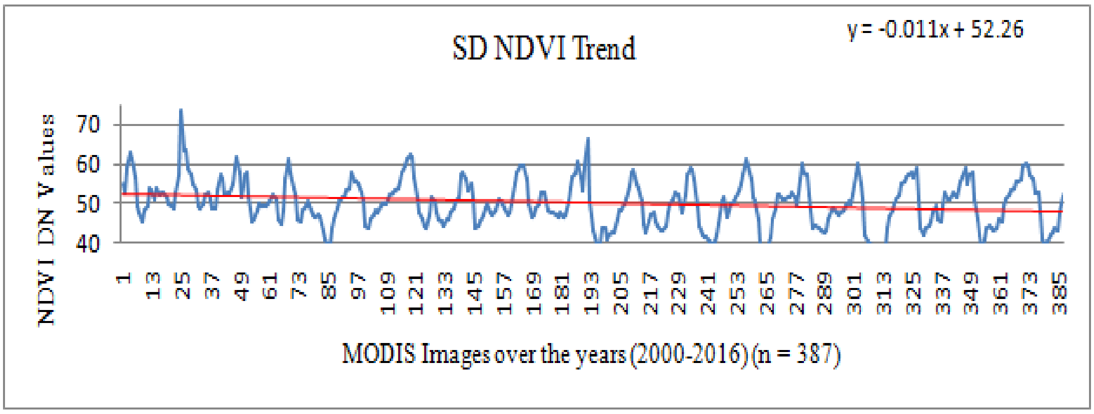


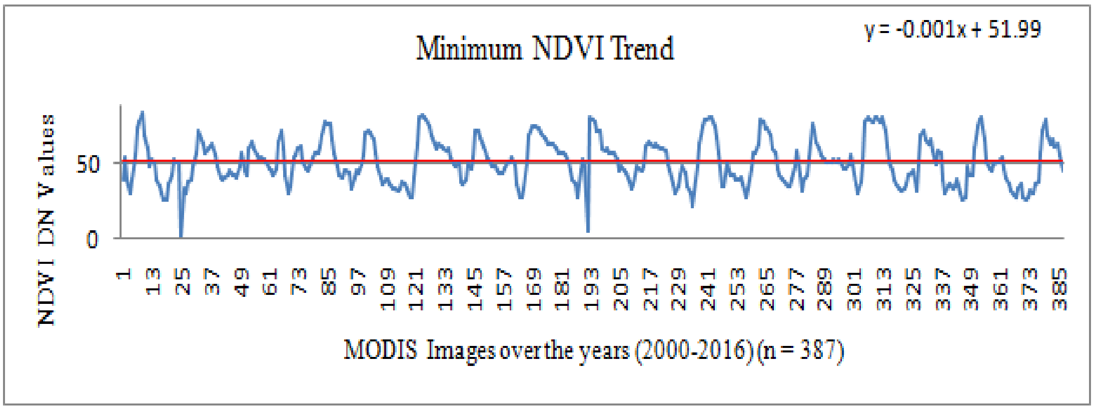


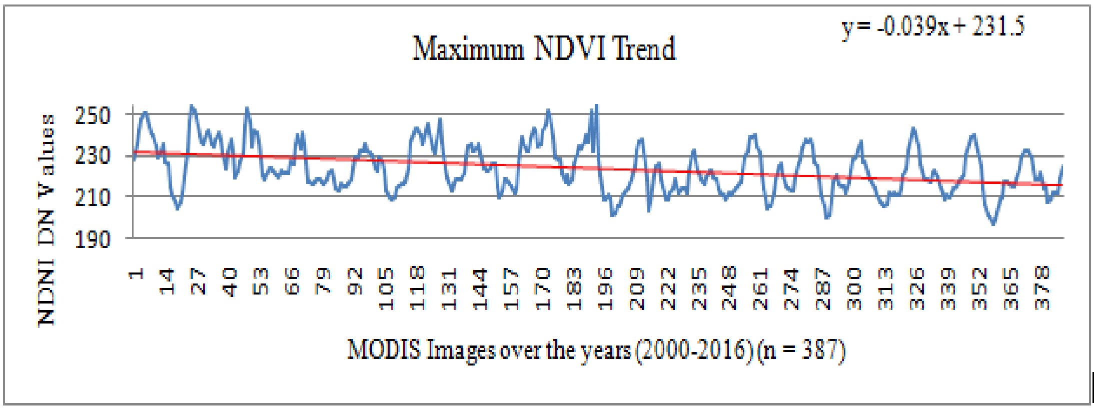

*Appendix 5*. *Yearly rainfall time-series for Addis Ababa station*

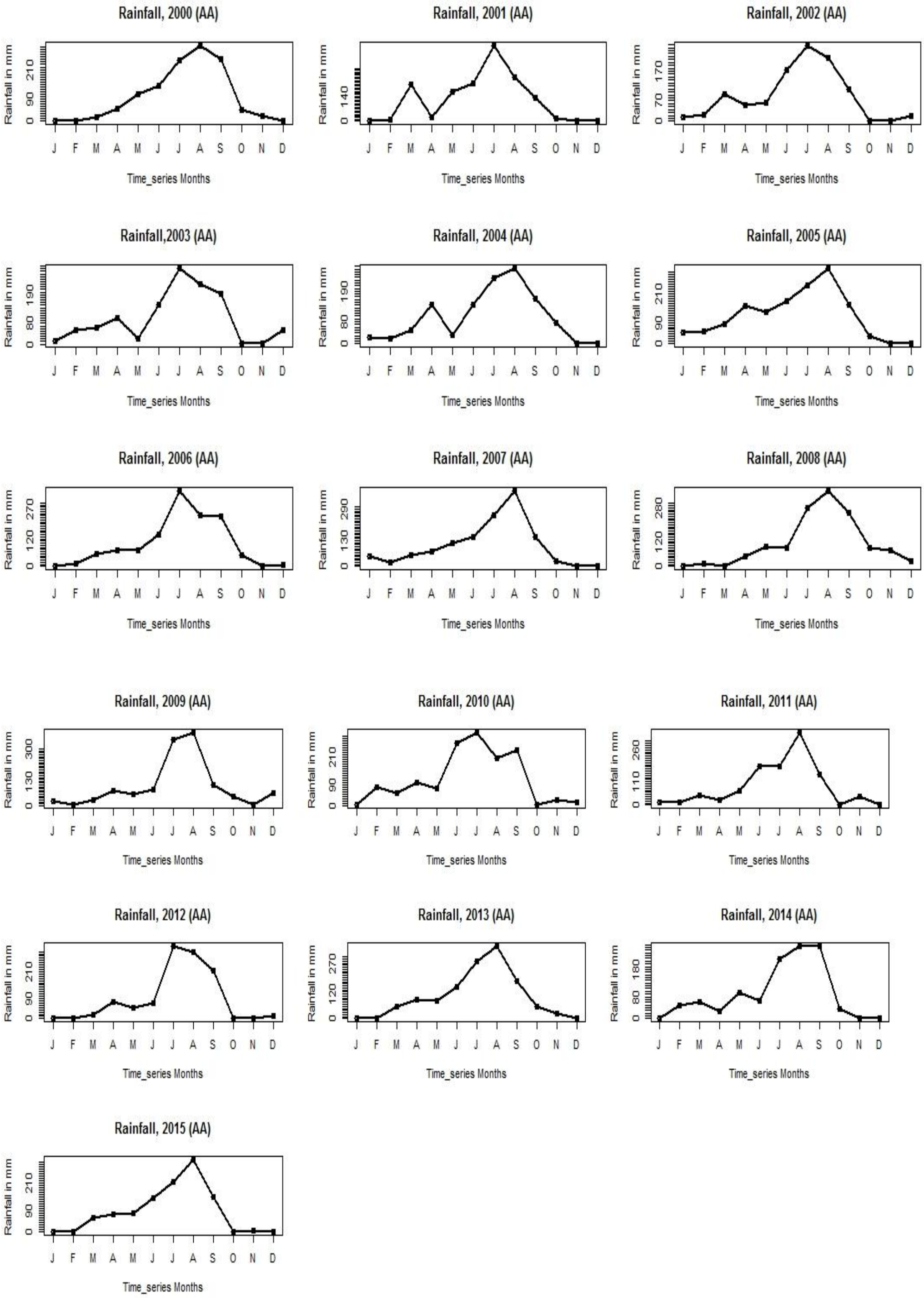

***Appendix 6****. Yearly rainfall time-series for Bole station*

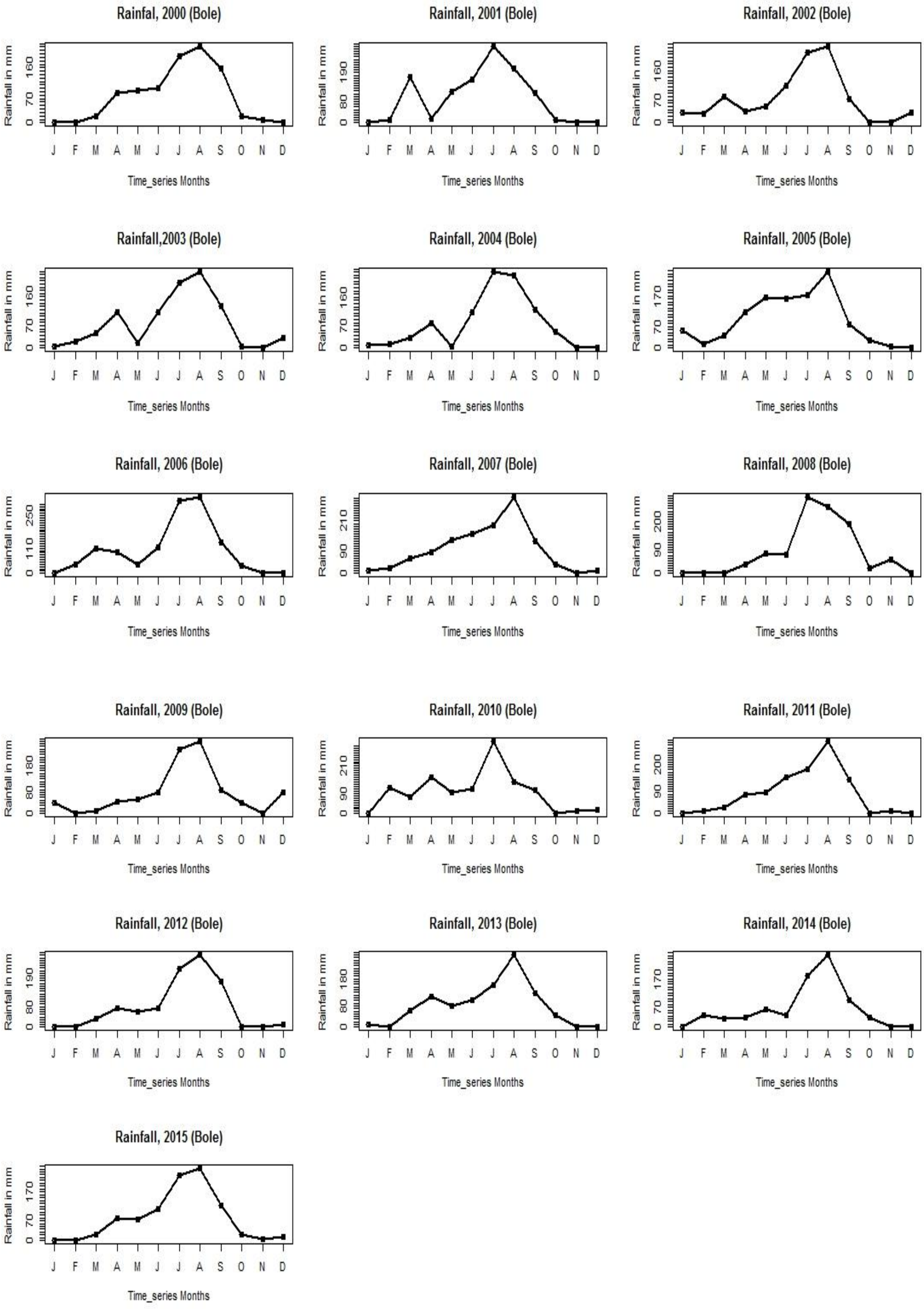

*__Appendix 7__. Linear trends of annual mean temperature in Addis Ababa (200-2015)*

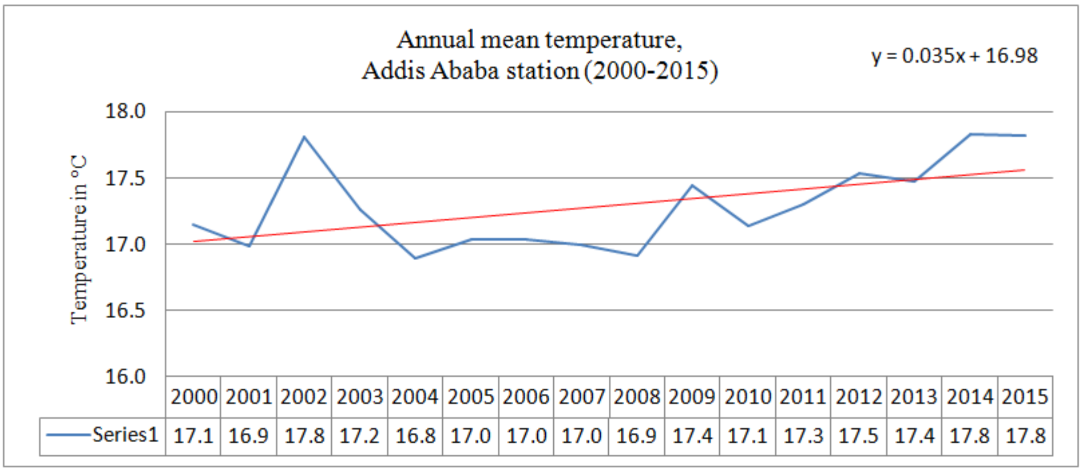


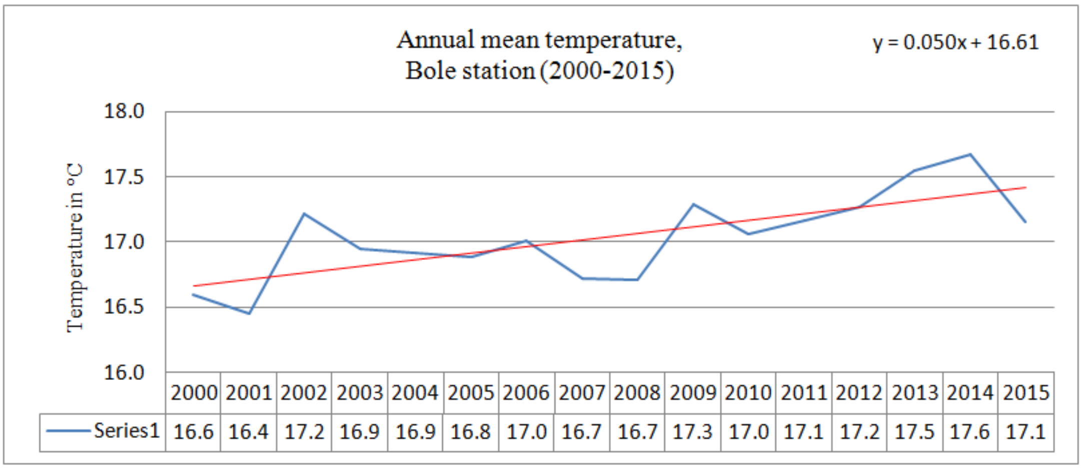

***Appendix 8***. *Correlation between monthly maximum NDVI and Rainfall for selected years*

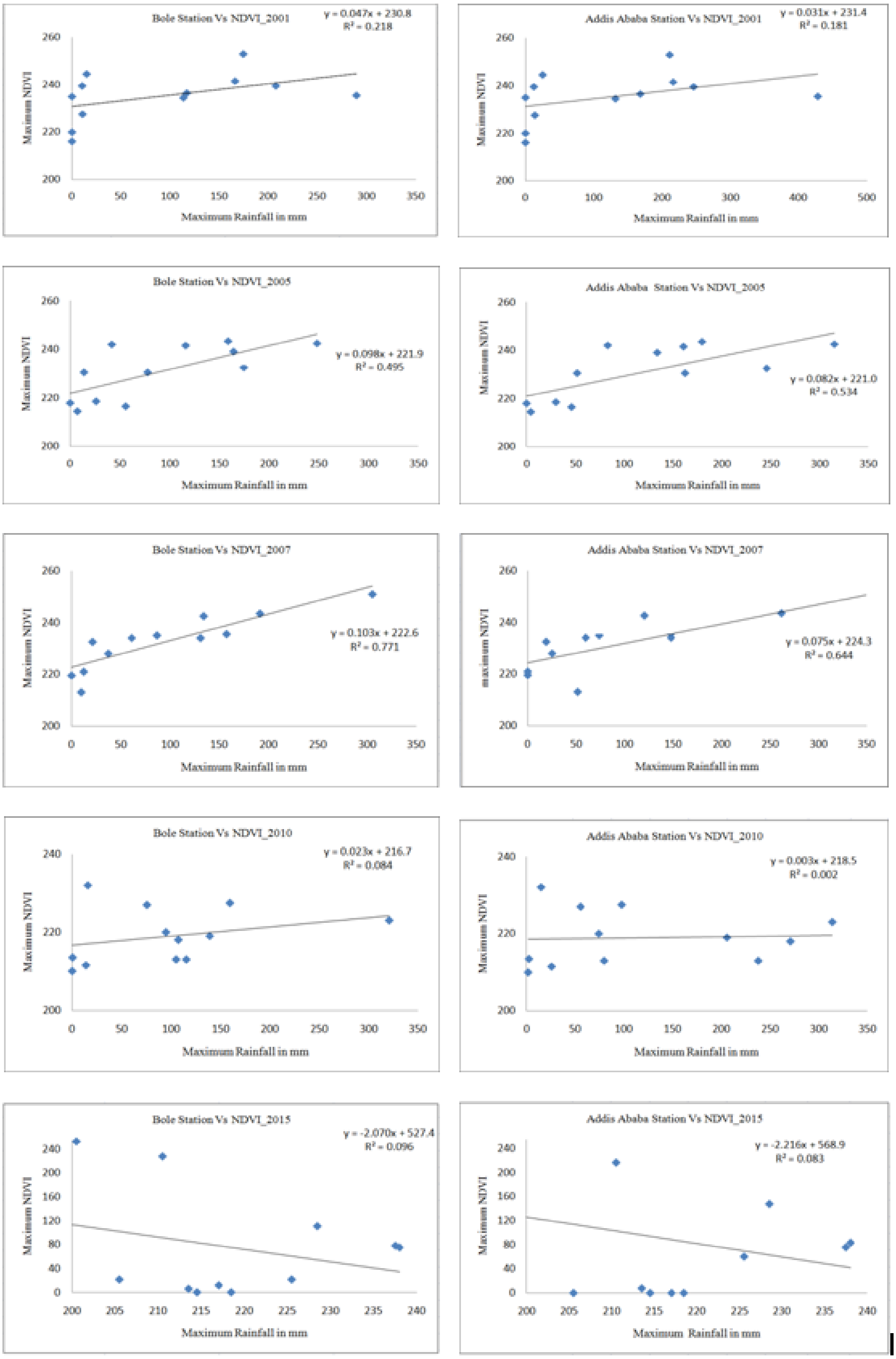

***Appendix 9***. *Control points for validation of LANDSAT ETM$^+$ 2000*

| X | Y | Landcover | X | Y | Landcover | X | Y | Landcover | X | Y | Landcover |
|---|---|---|---|---|---|---|---|---|---|---|---|
| 487391 | 975550 | Agriculture | 460992 | 1007580 | Vegetation | 470575 | 986642 | Agriculture | 474474 | 985909 | Builtup |
| 488449 | 976270 | Agriculture | 460730 | 1008900 | Vegetation | 470880 | 987065 | Agriculture | 476513 | 990027 | Builtup |
| 489507 | 978598 | Agriculture | 464802 | 1007250 | Vegetation | 471066 | 982849 | Agriculture | 473764 | 990067 | Builtup |
| 490777 | 979741 | Agriculture | 463337 | 1005560 | Vegetation | 470202 | 983272 | Agriculture | 475105 | 990013 | Builtup |
| 486121 | 982112 | Agriculture | 467097 | 1005780 | Vegetation | 470236 | 983780 | Agriculture | 475909 | 988914 | Builtup |
| 482438 | 987319 | Agriculture | 467435 | 1005180 | Vegetation | 482191 | 980969 | Agriculture | 465221 | 994466 | Builtup |
| 480575 | 985710 | Agriculture | 464243 | 1005690 | Vegetation | 479075 | 982916 | Agriculture | 458770 | 985145 | Builtup |
| 478035 | 987234 | Agriculture | 459891 | 1002030 | Vegetation | 479499 | 984999 | Agriculture | 457053 | 984622 | Builtup |
| 486205 | 985329 | Agriculture | 460526 | 1002970 | Vegetation | 482682 | 984728 | Agriculture | 462552 | 987331 | Builtup |
| 485359 | 987912 | Agriculture | 457106 | 998217 | Vegetation | 480345 | 989910 | Agriculture | 472235 | 992172 | Builtup |
| 488703 | 984991 | Agriculture | 460391 | 999309 | Vegetation | 477663 | 1008600 | Agriculture | 473978 | 995324 | Builtup |
| 478120 | 976736 | Agriculture | 461754 | 997040 | Vegetation | 477769 | 1005170 | Agriculture | 478565 | 992508 | Builtup |
| 470711 | 975974 | Agriculture | 474788 | 1000920 | Vegetation | 479695 | 1006000 | Agriculture | 477586 | 993084 | Builtup |
| 472489 | 976990 | Agriculture | 469675 | 1005710 | Vegetation | 479399 | 1000790 | Agriculture | 477398 | 996705 | Builtup |
| 472489 | 978683 | Agriculture | 473009 | 1007530 | Vegetation | 479039 | 1003480 | Agriculture | 470411 | 997765 | Builtup |
| 473759 | 978217 | Agriculture | 475813 | 1007880 | Vegetation | 480626 | 1001940 | Agriculture | 473308 | 1002120 | Builtup |
| 471304 | 976905 | Agriculture | 475840 | 1004520 | Vegetation | 462529 | 1008560 | Agriculture | 473817 | 1002930 | Builtup |
| 463134 | 976185 | Agriculture | 474226 | 1004280 | Vegetation | 458740 | 1008310 | Agriculture | 467527 | 1000180 | Builtup |
| 463938 | 975889 | Agriculture | 471474 | 1003430 | Vegetation | 459904 | 998295 | Agriculture | 473509 | 997389 | Builtup |
| 463853 | 978048 | Agriculture | 467400 | 1002720 | Vegetation | 461322 | 1004390 | Agriculture | 463947 | 1003910 | Builtup |
| 458011 | 977921 | Agriculture | 475549 | 1003540 | Vegetation | 457173 | 1005530 | Agriculture | 488030 | 1002350 | Builtup |
| 457588 | 976312 | Agriculture | 477851 | 1002590 | Vegetation | 456242 | 1008540 | Agriculture | 486117 | 1001390 | Builtup |
| 491488 | 992348 | Agriculture | 482095 | 1008440 | Vegetation | 457216 | 1008260 | Agriculture | 481672 | 996842 | Builtup |
| 491098 | 991028 | Agriculture | 477089 | 1007300 | Vegetation | 456708 | 1007520 | Agriculture | 482366 | 998679 | Builtup |
| 491030 | 990587 | Agriculture | 479534 | 1007080 | Vegetation | 460581 | 1000600 | Agriculture | 483839 | 995191 | Builtup |
| 491064 | 993483 | Agriculture | 481206 | 1003310 | Vegetation | 456560 | 995141 | Agriculture | 488310 | 991982 | Builtup |
| 490505 | 995362 | Agriculture | 464167 | 983545 | Vegetation | 459713 | 994400 | Agriculture | 486879 | 993269 | Builtup |
| 491301 | 996226 | Agriculture | 465649 | 981878 | Vegetation | 457597 | 987394 | Agriculture | 491688 | 993844 | Builtup |
| 491521 | 994838 | Agriculture | 468915 | 1007520 | Vegetation | 458740 | 988727 | Agriculture | 485888 | 997434 | Builtup |
| 487491 | 994346 | Agriculture | 466269 | 1004320 | Vegetation | 491574 | 985648 | Agriculture | 476161 | 992380 | Builtup |
| 487322 | 996362 | Agriculture | 475318 | 1006620 | Vegetation | 491415 | 983016 | Agriculture | 477354 | 992524 | Builtup |
| 487203 | 998072 | Agriculture | 477435 | 1006060 | Vegetation | 491508 | 987447 | Agriculture | 470116 | 995279 | Builtup |
| 488236 | 996649 | Agriculture | 465859 | 1007570 | Vegetation | 457562 | 1000150 | Agriculture | 474681 | 999593 | Builtup |
| 487999 | 995803 | Agriculture | 468876 | 1003990 | Vegetation | 457231 | 1002670 | Agriculture | 471506 | 1002460 | Builtup |
| 491606 | 997225 | Agriculture | 482779 | 977805 | Vegetation | 457906 | 1003940 | Agriculture | 474734 | 977802 | Builtup |
| 491792 | 999054 | Agriculture | 484632 | 977924 | Vegetation | 456781 | 1003270 | Agriculture | 458764 | 1001790 | water |
| 487949 | 1001040 | Agriculture | 491021 | 976058 | Vegetation | 459970 | 1004330 | water | 459043 | 1002080 | water |
| 489252 | 1001810 | Agriculture | 456400 | 985954 | Vegetation | 467584 | 975165 | water | 458827 | 1002570 | water |
| 489845 | 1001930 | Agriculture | 461983 | 990372 | Vegetation | 467393 | 975864 | water | 459818 | 1003030 | water |
| 487237 | 1003170 | Agriculture | 462949 | 989592 | Vegetation | 467901 | 976778 | water | 459443 | 1002760 | water |
| 487711 | 1004390 | Agriculture | 461414 | 989909 | Vegetation | 468155 | 976162 | water | 459481 | 1002420 | water |
| 486983 | 1005780 | Agriculture | 460845 | 1001420 | Vegetation | 469070 | 976632 | water | 459215 | 1002440 | water |
| 491505 | 1008330 | Agriculture | 478313 | 989002 | Vegetation | 468993 | 977229 | water | 460339 | 1002140 | water |
| 491555 | 1007520 | Agriculture | 471811 | 1006750 | Vegetation | 468485 | 976981 | water | 460529 | 1001920 | water |
| 457011 | 977515 | Agriculture | 481998 | 1007440 | Vegetation | 468676 | 976372 | water | 459812 | 1002450 | water |
| 458603 | 979462 | Agriculture | 481462 | 977608 | Builtup | 472194 | 975152 | water | 459735 | 1002820 | water |
| 458349 | 982205 | Agriculture | 478685 | 979526 | Builtup | 472460 | 975679 | water | 460002 | 1003990 | water |
| 459467 | 982730 | Agriculture | 475802 | 976629 | Builtup | 472753 | 975216 | water | 460034 | 1004680 | water |
| 467019 | 987980 | Agriculture | 471591 | 978815 | Builtup | 477446 | 983197 | water | 460097 | 1004330 | water |
| 467087 | 989029 | Agriculture | 487255 | 986701 | Builtup | 472947 | 985740 | water | 474397 | 976734 | water |
| 467781 | 986405 | Agriculture | 475225 | 983536 | Builtup | 472947 | 985740 | water | 489319 | 991988 | water |
| 490886 | 992883 | water | 489830 | 998585 | water | 474806 | 990787 | water | 490014 | 991208 | water |

***Appendix 10.*** *Control points for validation of LANDSAT 8 (OLI) 2017*

| X | Y | Landcover | X | Y | Landcover | X | Y | Landcover | X | Y | Landcover | X | Y | Landcover |
|---|---|---|---|---|---|---|---|---|---|---|---|---|---|---|
| 466450 | 1002032 | Agriculture | 475446 | 1000942 | Builtup | 468339 | 1056632 | Vegetation | 466187 | 1002610 | Builtup | 466990 | 994829 | Builtup |
| 468720 | 1006165 | Agriculture | 475445 | 1000921 | Builtup | 468330 | 1005614 | Vegetation | 467783 | 1002599 | Builtup | 466705 | 995004 | Builtup |
| 468639 | 1005134 | Agriculture | 475800 | 1000333 | Builtup | 470748 | 1003404 | Vegetation | 467740 | 1002620 | Builtup | 466603 | 994736 | Builtup |
| 468634 | 1005115 | Agriculture | 475641 | 999967 | Builtup | 472723 | 1000746 | Vegetation | 467729 | 1002610 | Builtup | 465903 | 994007 | Builtup |
| 487389 | 997014 | Agriculture | 475492 | 999713 | Builtup | 472719 | 1000740 | Vegetation | 467483 | 1002779 | Builtup | 465634 | 995309 | Builtup |
| 487383 | 996947 | Agriculture | 476219 | 999576 | Builtup | 473895 | 1004584 | Vegetation | 468362 | 1006050 | Builtup | 466138 | 995141 | Builtup |
| 487874 | 997015 | Agriculture | 476212 | 999647 | Builtup | 474053 | 1004492 | Vegetation | 468417 | 1005975 | Builtup | 467704 | 996329 | Builtup |
| 461265 | 991657 | Agriculture | 476287 | 998079 | Builtup | 473750 | 1004054 | Vegetation | 468612 | 1006088 | Builtup | 467427 | 999284 | Builtup |
| 467128 | 996984 | Agriculture | 480181 | 997311 | Builtup | 473738 | 1004043 | Vegetation | 468055 | 1006014 | Builtup | 468564 | 996598 | Builtup |
| 466782 | 992152 | Agriculture | 482548 | 998170 | Builtup | 473756 | 1004075 | Vegetation | 468697 | 1005169 | Builtup | 468007 | 992838 | Builtup |
| 467622 | 1002672 | Agriculture | 483477 | 998510 | Builtup | 473683 | 1004113 | Vegetation | 472488 | 1000411 | Builtup | 468193 | 992979 | Builtup |
| 467770 | 1002570 | Agriculture | 483605 | 996966 | Builtup | 474246 | 1001290 | Vegetation | 472803 | 1000605 | Builtup | 487377 | 997229 | Builtup |
| 467778 | 1002572 | Agriculture | 486248 | 996949 | Builtup | 474296 | 1001321 | Vegetation | 472739 | 1000742 | Builtup | 486816 | 998033 | Builtup |
| 468697 | 1006154 | Agriculture | 486633 | 1000921 | Builtup | 474311 | 1001231 | Vegetation | 473920 | 1004521 | Builtup | 486273 | 997157 | Builtup |
| 468298 | 1005615 | Agriculture | 485431 | 999685 | Builtup | 474381 | 1001090 | Vegetation | 474020 | 1004493 | Builtup | 485811 | 997937 | Builtup |
| 469640 | 1003891 | Agriculture | 482276 | 998813 | Builtup | 474406 | 1001105 | Vegetation | 474003 | 1004505 | Builtup | 485945 | 997627 | Builtup |
| 469655 | 1003883 | Agriculture | 476780 | 997811 | Builtup | 474257 | 1001347 | Vegetation | 473890 | 1004548 | Builtup | 486020 | 1001170 | Builtup |
| 474032 | 1004485 | Agriculture | 475607 | 998523 | Builtup | 476861 | 1002101 | Vegetation | 473869 | 1004309 | Builtup | 485210 | 998933 | Builtup |
| 473805 | 1004415 | Agriculture | 475041 | 998890 | Builtup | 476850 | 1002113 | Vegetation | 473192 | 1003305 | Builtup | 483622 | 998917 | Builtup |
| 473863 | 1004331 | Agriculture | 474947 | 999096 | Builtup | 476980 | 1001154 | Vegetation | 473829 | 1000830 | Builtup | 482291 | 998824 | Builtup |
| 473716 | 1004086 | Agriculture | 474282 | 999096 | Builtup | 476230 | 999655 | Vegetation | 474145 | 1001269 | Builtup | 482152 | 998915 | Builtup |
| 473526 | 1004107 | Agriculture | 473951 | 999709 | Builtup | 488748 | 998534 | Vegetation | 474264 | 1001362 | Builtup | 484302 | 1000160 | Builtup |
| 474263 | 1001358 | Agriculture | 473661 | 999534 | Builtup | 483456 | 998528 | Vegetation | 474302 | 1001337 | Builtup | 476843 | 1002151 | Builtup |
| 474339 | 1001168 | Agriculture | 473423 | 999813 | Builtup | 483501 | 998539 | Vegetation | 474338 | 1001164 | Builtup | 476755 | 1001004 | Builtup |
| 476890 | 1002127 | Agriculture | 473370 | 999755 | Builtup | 487378 | 996903 | Vegetation | 474394 | 1001104 | Builtup | 477079 | 1001164 | Builtup |
| 476891 | 1001927 | Agriculture | 473302 | 999701 | Builtup | 487875 | 997044 | Vegetation | 474403 | 1001110 | Builtup | 477864 | 997577 | Builtup |
| 476947 | 1001118 | Agriculture | 473271 | 999632 | Builtup | 485415 | 999656 | Vegetation | 474367 | 1001133 | Builtup | 476638 | 999179 | Builtup |
| 476219 | 999585 | Agriculture | 473290 | 999707 | Builtup | 483734 | 998945 | Vegetation | 474361 | 1001168 | Builtup | 477340 | 998686 | Builtup |
| 483437 | 998582 | Agriculture | 473267 | 999617 | Builtup | 479705 | 998328 | Vegetation | 474379 | 1001245 | Builtup | 472533 | 1000464 | Builtup |
| 479614 | 998428 | Agriculture | 473292 | 999558 | Builtup | 479647 | 998339 | Vegetation | 474371 | 1001252 | Builtup | 472776 | 1000749 | Builtup |
| 473420 | 999677 | Agriculture | 473337 | 999552 | Builtup | 479311 | 998339 | Vegetation | 474358 | 1001281 | Builtup | 470652 | 1001616 | Builtup |
| 467942 | 994052 | Agriculture | 473382 | 999544 | Builtup | 479302 | 998398 | Vegetation | 474282 | 1001275 | Builtup | 466285 | 1000461 | Builtup |
| 466861 | 994924 | Agriculture | 473622 | 999681 | Builtup | 473503 | 999536 | Vegetation | 474268 | 1001289 | Builtup | 467513 | 999322 | Builtup |
| 468382 | 998088 | Agriculture | 469974 | 1001054 | Builtup | 473405 | 999772 | Vegetation | 473700 | 999825 | Builtup | 472889 | 999682 | Builtup |
| 468205 | 991970 | Agriculture | 466297 | 1001893 | Builtup | 473363 | 999774 | Vegetation | 476857 | 1002019 | Builtup | 466215 | 1002781 | Vegetation |
| 472529 | 999987 | Builtup | 466080 | 1001141 | Builtup | 473305 | 999691 | Vegetation | 476836 | 1002155 | Builtup | 466191 | 1002772 | Vegetation |
| 472678 | 999599 | Builtup | 465914 | 1001661 | Builtup | 473364 | 999563 | Vegetation | 476851 | 1002157 | Builtup | 466432 | 1002083 | Vegetation |
| 466310 | 1002748 | Builtup | 466304 | 999727 | Builtup | 473394 | 999642 | Vegetation | 477026 | 1001153 | Builtup | 467781 | 1002580 | Vegetation |
| 466217 | 1002766 | Builtup | 466154 | 999811 | Builtup | 473492 | 999677 | Vegetation | 476792 | 1001079 | Builtup | 467777 | 1002587 | Vegetation |
| 475961 | 1000155 | Water | 477522 | 1000945 | Water | 483683 | 998964 | Water | 476813 | 1001317 | Builtup | 467778 | 1002551 | Vegetation |
| 475710 | 999861 | Water | 476696 | 1000172 | Water | 483685 | 998937 | Water | 473585 | 999665 | Vegetation | 466421 | 1000445 | Water |
| 475601 | 998868 | Water | 477208 | 998797 | Vegetation | 486777 | 1001225 | Water | 472752 | 999807 | Vegetation | 468387 | 992044 | Water |
| 481445 | 997737 | Water | 472903 | 999665 | Vegetation | 466568 | 1002249 | Water | 471196 | 1000958 | Vegetation | 475626 | 999951 | Water |
| 481827 | 997868 | Water | 473603 | 999747 | Vegetation | 466463 | 1002038 | Water | 468567 | 1000792 | Vegetation | 468290 | 993696 | Water |
| 480367 | 998813 | Water | 472869 | 999661 | Water | 470723 | 1003359 | Water | 467737 | 996343 | Vegetation | 475626 | 999940 | Water |
| 480368 | 998440 | Water | 472880 | 999665 | Water | 474394 | 1001243 | Water | 468558 | 996868 | Vegetation | 467212 | 996970 | Water |
| 479569 | 998433 | Water | 466588 | 1002655 | Water | 474283 | 1001285 | Water | 483734 | 998945 | Vegetation | 466667 | 999968 | Water |
| 472064 | 1001187 | Water | 466550 | 1001767 | Water | 474282 | 1001287 | Water | 466832 | 992146 | Water | 471196 | 1000958 | Water |
| 474286 | 1001286 | Water | 468322 | 993384 | Water | 466995 | 997817 | Water | | | | | | |

**Department of Physical Geography and Ecosystem Science, Lund University**

Lund University GEM thesis series are master theses written by students of the international master program on Geo-information Science and Earth Observation for Environmental Modelling and Management (GEM). The program is a cooperation of EU universities in Iceland, the Netherlands, Poland, Sweden and UK, as well a partner university in Australia. In this series only master thesis are included of students that performed their project at Lund University. Other theses of this program are available from the ITC, the Netherlands (www.gem-msc.org or www.itc.nl).

The student thesis reports are available at the Geo-Library, Department of Physical Geography and Ecosystem Science, University of Lund, Sölvegatan 12, S-223 62 Lund, Sweden. Report series started 2013. The complete list and electronic versions are also electronic available at the LUP student papers (https://lup.lub.lu.se/student-papers/search/) and through the Geo-library (www.geobib.lu.se).

1 SoheilaYouneszadehJalili (2013) The effect of land use on land surface temperature in the Netherlands

2 Oskar Löfgren (2013) Using Worldview-2 satellite imageryto detect indicators of high speciesdiversity in grasslands

3 Yang Zhou (2013) Inter-annual memory effects between Soil Moisture and NDVI in the Sahel

4 Efren Lopez Blanco (2014) Assessing the potential of embedding vegetation dynamics into a fire behaviour model:LPJ-GUESS-FARSITE

5 Anna Movsisyan(2014) Climate change impact on water and temperature conditions of forest soils: A case study related to the Swedish forestry sector

6 Liliana Carolina Castillo Villamor (2015) Technical assessment of GeoSUR and comparison with INSPIRE experience in the context of an environmental vulnerability analysis using GeoSUR data

7 Hossein Maazallahi (2015)Switching to the “Golden Age of Natural Gas” with a Focus on Shale Gas Exploitation: A Possible Bridge to Mitigate Climate Change?

8 Mohan Dev Joshi (2015) Impacts of Climate Change on *Abiesspectabilis*: An approach integrating Maxent Model (MAXent) and Dynamic Vegetation Model (LPJ-GUESS)

9 AltaafMechiche-Alami(2015) Modelling future wheat yields in Spain with LPJ-GUESS and assessing the impacts of earlier planting dates

10 KoffiUnwana Saturday (2015) Petroleum activities, wetland utilization and livelihood changes in Southern AkwaIbom State, Nigeria: 2003-2015

11 José Ignacio Díaz González (2016) Multi-objective optimisation algorithms for GIS-based multi-criteria decision analysis: an application for evacuation planning

12 Gunjan Sharma (2016) Land surface phenology as an indicator of performance of conservation policies like Natura2000

13 Chao Yang (2016) A Comparison of Four Methods of Diseases Mapping

14 Xinyi Dai (2016) Dam site selection using an integrated method of AHP and GIS for decision making support in Bortala, Northwest China

15 JialongDuanmu (2016) A multi-scale based method for estimating coniferous forest aboveground biomass using low density airborne LiDAR data

16 Tanyaradzwa J. N. Muswera (2016) Modelling maize (Zea Mays L.) phenology using seasonal climate forecasts

17 Maria Angela Dissegna (2016) Improvement of the GPP estimations for Sudan using the evaporative fraction as water stress factor

18 Miguel G. Castro Gómez (2017) Joint use of Sentinel-1 and Sentinel-2 for land cover classification: A machine learning approach

19 Krishna Lamsal (2017) Identifying potential critical transitions in a forest ecosystem using satellite data

20 MaimoonaZehraJawaid (2017) Glacial lake flood hazard assessment and modelling: a GIS perspective

21 Tracy Zaarour(2017) Application of GALDIT index in the Mediterranean region to assess vulnerability to sea water intrusion

22 StephaniaZabala (2017) Comparison of multi-temporal and multispectral Sentinel-2 and UAV (unmanned aerial vehicle) imagery for crop type mapping

23 Ximena Tagle (2017) Radiometric calibration of unmanned aerial vehicle remote sensing imagery for vegetation mapping

24 Tesfaye Gebeyehu Admasu (2017) Monitoring trends of greenness and LULC (land use/land cover) change in Addis Ababa and its surrounding using MODIS time-series and LANDSAT data